Review on" Some insights into the condensing vapors driving new particle growth to CCN sizes on the basis of hygroscopicity measurements" by Z. J. Wu et al.

The authors present a case study on atmospheric new particle formation at a continental location, addressing the question of the composition of the condensing vapors in NPF growth indirectly through HTDMA and AMS measurements. While the paper discusses only three NPF events it provides an interesting view into the composition of the growth in NPF, which is still not very well characterized. I recommend the manuscript for publication after the following issues have been addressed.

****

The authors greatly appreciate that the reviewer spent lots of time to read this manuscript and provide these constructive suggestions. We modified the manuscript according to the comments point by point.

****

My main concern is that the AMS data is underutilized. The paper seems to have a general mindset that only sulfuric acid and organics can contribute to the growth (e.g. page 8413, rows 1-2). Does the AMS data support this? What is the contribution of e.g. ammonium to the growth? For instance Zhang et al. (2004) combined AMS and SMPS in order to get an insight into chemistry of new particle formation and growth. I strongly recommend applying the Zhang et al. (2004) approach in your data set. This way you could compare the AMS and hygroscopicity implications on the composition.

Response:

By following the referee's comments, we carefully read Zhang's EST paper and made a deeper analysis of size-resolved AMS data. The particle volume size distributions were calculated firstly. Based on the particle volume size distribution, the size-resolved particle mass concentrations were estimated using a particle density of 1400 kg/m^3. The results are shown in the Fig.1. The mass concentrations of particles below 50 nm in mobility diameter are lower than 1 µg/m^3. We tried to integrate the AMS size distribution data to calculate the mass concentrations of organic, sulfate, nitrate, and ammonium. However, the signals for particle size smaller than 50 nm in AMS dataset are too noisy and cannot be used to analyze the chemical composition of new particles. The mass concentrations of particles below 100 nm in mobility diameters are several µg/m^3, as displayed in the Fig.1. And, the signals for this size range are much better. Considering the accuracy of size-resolved particle mass concentration detected by AMS and the transmission efficiency of aerodynamic lenses (100 nm in Dva) (Canagaratna et al., 2007), the chemical composition of 30-100 nm particles is chosen to perform the further analysis.

In addition, the fragment m/z 44 and 57 mass concentrations of 30-100 nm particles were calculated. m/z 44 (CO_2^+ ion fragment) is a good tracer for photochemically formed secondary organic aerosol, while m/z 57 ($C_4H_9^+$) is generally associated with primary organics from combustion sources (Zhang et al., 2004). An analysis on both chemical composition and fragment m/z 44 and 57 was added into the manuscript.

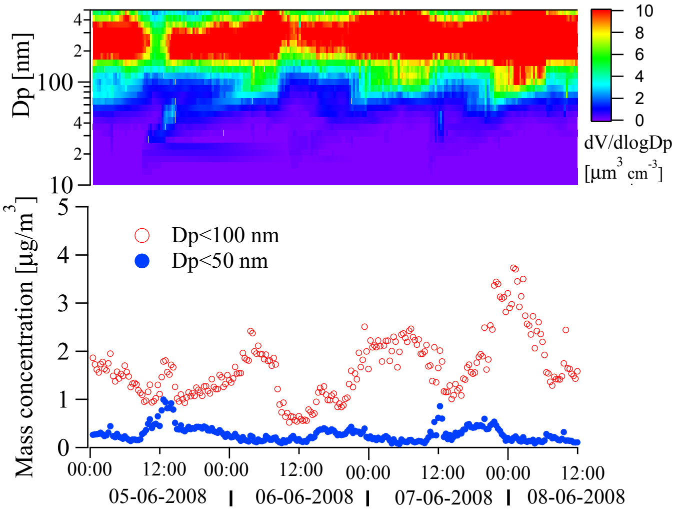

Fig.1: Particle volume size distribution and estimated mass concentration of particles smaller than 50 nm and 100 nm in mobility diameter.

Modification in the MS:

A new plot (Fig.3 in the MS) and some discussions were added into the section 4.2.

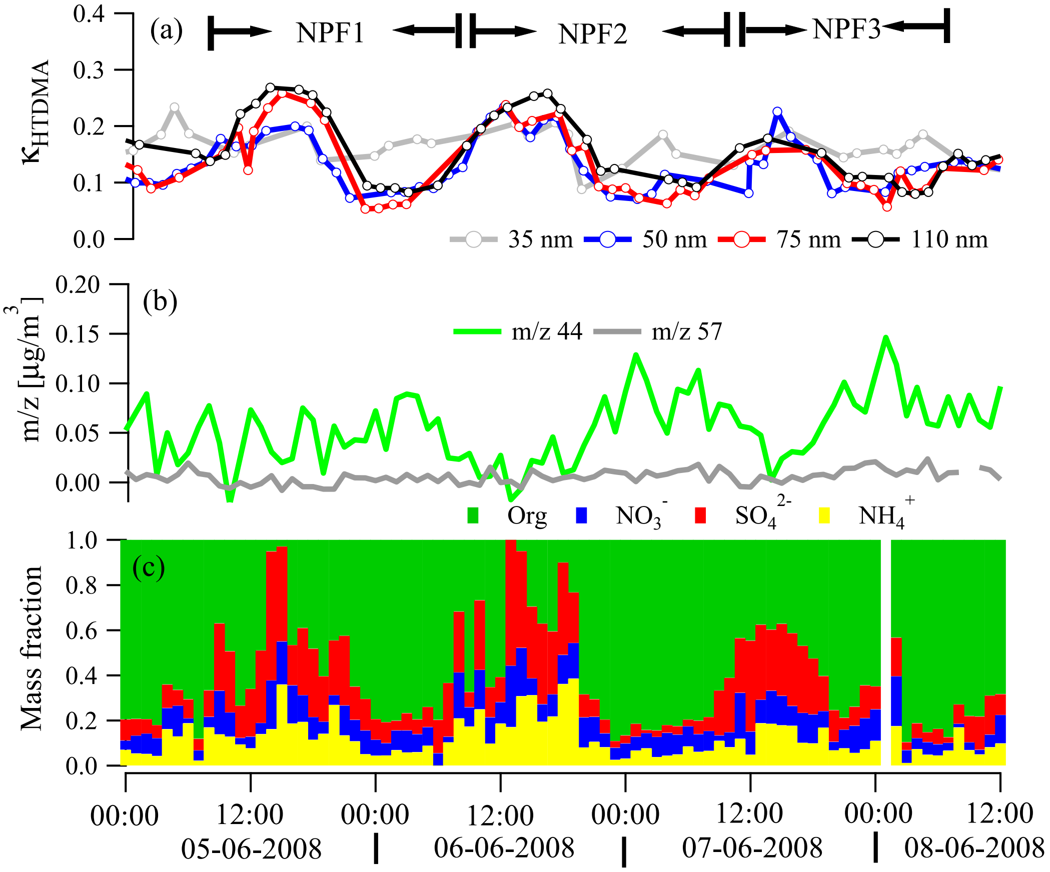

Fig.3: Size-resolved particle hygroscopicity (a), m/z 44 and 57 mass concentrations in 30-100 nm particles (b), and mass fraction of organic, sulfate, nitrate, and ammonium in 30-100 nm particles (c).

"As displayed in Fig.3 (c), the sulfate and ammonium were dominated in the inorganic mass fraction in 30-100 nm particles and obviously increased during the particle formation period (indicated by grey dashed line in Fig.1). While, the nitrate accounted for a minor fraction, which also observed by Zhang et al. in Pittsburgh (Zhang et al., 2004). They found nitrate contributed the least to the new particle growth. After 3:00pm on each day, the organic mass fraction increased and reached its maximum at midnight, indicating that organics played a key role in the particle growth at a later time of the NPF event. The mass fraction of ion fragments m/z 44 and 57 in 30-100 nm particles are shown in the Fig. 3(b). The m/z 44 (CO_2^+ ion fragment) is a tracer for secondary organic aerosol，while m/z 57 ($C_4H_9^+$) is generally associated with primary organics from combustion sources (Zhang et al., 2004). The m/z 57 mass concentration is close to zero during the events. Compared m/z 57, the m/z 44 mass concentration are considerable, indicating that the organics contributing to particle growth was mainly secondary organic species."

****

Minor comments

page 8405, row 14 "Freshly formed particles are about several nanometers in diameter" Can you give more precise size, maybe with a reference? "About several nanometers" sound quite large for a freshly formed particle to me.

Response:

Freshly formed particles are about 1 nanometer in diameter (Kulmala et al., 2012). It was corrected in the MS.

****

Page 8405, row 27-29 Please clarify the last sentence.

Response:

The sentence is deleted from the manuscript.

****

page 8408 The methods for aerosol particle formation and growth rate analysis are not described at all. Please add a section in Chapter 3 on these.

Response

One section (3.4) was added in the texts to describe the method.

Modification in the MS:

3.4 Calculation of particle formation and growth rate

Assuming a constant particle source during a time period of t, the particle formation rate (Jnuc) can be expressed as (Dal Maso et al., 2005):

$$J_{nuc} = \frac{dN_{nuc}}{dt} + F_{coag} + F_{growth} \qquad [10]$$

In this study, Nnuc is the number concentration of nucleation mode particles ranging from 3 nm to 25 nm. Fgrowth is the flux of particles out of the specified size range (3-25 nm). The newly formed particles rarely grew beyond 25 nm before formation ended, and Fgrowth can be neglected. Fcoag represents a loss of formed particles due to coagulation to the preexisting particle population. It can be calculated from the following equation:

$$F_{coag} = CoagS_{nuc}N_{nuc} \qquad [11]$$

where $CoagS_{nuc}$ is the coagulation sink of particles in the nucleation mode. The detailed calculation of coagulation sink is given in Deal Maso et al. (2005).

The observed particle growth rate (GR) can be expressed as:

$$\mathrm{GR} = \frac{\Delta \mathrm{D_m}}{\Delta \mathrm{t}} \qquad [12]$$

where Dm is a mean geometric diameter of log-normal ultrafine particle mode, which has been fitted to the number size distribution (Heintzenberg, 1994). GR means evolution of the mean diameter within a time period Δt.

****

page 8411, row 16-17 Please give a reference (or a detailed description) for the hygroscopic growth parameterization.

Response:

The method of hygroscopic growth parameterization originates from Laakso et al., 2004.

Modification in the MS:

One reference was added into the MS "For this adjustment, an empirical growth law based on one year of hygroscopicity measurements at Melpitz was used (Refer to Laakso et al., 2004)."

****

page 8412, row 1-2 Please include a short discussion on the accuracy of the H_2SO_4 estimate.

Response:

The accuracy of simulated H_2SO_4 concentration is estimated as follow: Percentage error = abs ($[H_2SO_4]_{measured}$ - $[H_2SO_4]_{simulated}$) * 100 / $[H_2SO_4]_{simulated}$. Here, $[H_2SO_4]_{measured}$ is the sulfuric acid concentration measured during 9-day measurements for EUCAARI-2008. The percentage error is around 40%.

These sentences were added into the MS.

****

page 8412, row 19 "where $[H_2SO_4]$det is the median value from the measured sulfuric acid concentration" Do you mean the estimated H2SO4 or did you have direct measurements as well?

Response:

$[H_2SO_4]_{det}$ is wrong. The H_2SO_4 concentration is estimated one. It was corrected in the MS.

Modification in the MS:

$[H_2SO_4]_{det}$ is modified to $[H_2SO_4]_{meas}$.

****

page 8413, row 13 Please indicate GR size range.

Response:

The observed particle growth rate (GR) can be expressed as:

$$\mathrm{GR} = \frac{\Delta D_m}{\Delta t}$$

where D_m is a mean geometric diameter of log-normal ultrafine particle mode, which has been fitted to the number size distribution (Heintzenberg, 1994). GR means evolution of the mean diameter within a time period Δt. The evolution of mean geometric diameter during NPF event is displayed in the following Fig.1 (a) (in the MS) as white circles. The period during which the observed GR is calculated is marked by NPF1, NPF2, and NPF3.

Modification in the MS:

"These events are the best cases which showed clear particle bursts and subsequent growth process during the entire field campaign. The starting and ending time for each event were marked in the Fig.1 (a) as NPF1, NPF2, and NPF3. "

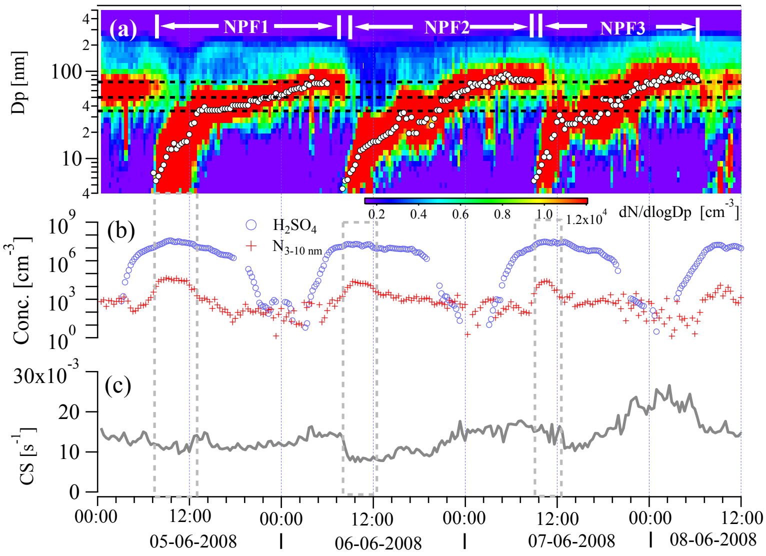

Fig. 1: Particle number size distribution, 3-10 nm particle number concentration, H_2SO_4 concentration, condensation sink (CS) during the NPF events. The starting and ending time of the events were marked in the upper place of panel (a) by NPF1, NPF2, and NPF3. The grey dashed lines indicated the time period of particle formation.

"As indicated by the white circle in the Fig.1 (a), the mean geometric diameter (D_m) of log-normal ultrafine particle mode increased to around 100 nm within 24 hours. Over the time period from the beginning to the end of the NPF events as marked in Fig.1 (a), the average GR_{obs}s were respectively 2.8, 3.6, and 4.4 nm h^{-1} for NPF events on June 5th, 6th, and 7th, 2008."

****

page 8415, row 7-8 "This was consistent with the variations in particle hygroscopic growth at RH= 90% above-mentioned." Please clarify this sentence.

Modification in the MS:

This was consistent with the variations in particle hygroscopic growth at RH= 90% displayed in the Fig. 3 (a))

****

page 8416, row 22-24 “At Melpitz, biological activities produced a lot of biogenic volatile organic compounds (BVOCs) and lead to an organic-rich environment during summertime.” Can you give a reference to support this statement?

Response:

The VOCs measurements performed at Melpitz research station showed that VOCs are mainly biogenic volatile organic compounds. The following figure copied from a supplementary material of a recent publication (Mutzel et al., 2015) displayed the VOCs concentration during summertime at Melpitz station. It is very clear that the BVOCs are dominated in the atmosphere of Melpitz.

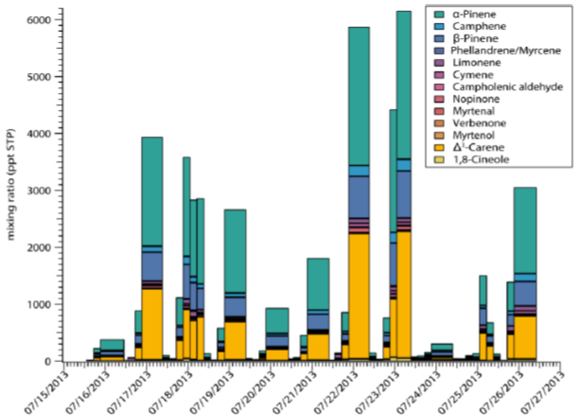

Figure S5. Time variation of the different VOC compounds sampled by TENAX cartridges. The width of each bar is covering the complete sampling period of each cartridge.

Modification in the MS:

At Melpitz, biogenic volatile organic compounds (BVOCs) emitted from biological activities are dominate volatile organic compounds (Mutzel et al., 2015) and lead to an organic-rich environment during summertime. The oxidation products of BVOCs may be responsible for the new particle growth.

****

page 8417, row 14-15 “The observation showed that sulfuric acid is a key species of atmospheric nucleation.” In my opinion this has not been shown. For instance analysis similar to Sihto et al. (2006) could be used to back up this statement.

Response:

Nucleation mechanism is not concerned in this work. This sentence is deleted from the MS.

****

page 8417, row 16 “CC” should probably be CCN?

Response:

It was corrected.

****

page 8417, row 26 “decline” do you mean increase?

Response:

Yes, it was corrected.

****

page 8418, row 1-4 "Our results implied that the CCN production associated with atmospheric nucleation may be overestimated if assuming that new particles can serve as CCN in case they grow to a fixed particle size, which was used in some previous studies, especially for organic-rich environments." Please quantify the error of the fixed size approach in your case for a few typical threshold sizes. This would be valuable information for evaluating the uncertainty in other studies that did not have hygroscopicity measurements available.

Response:

In our case, the mean critical diameter is around 50 nm at SS=0.6%. Assuming a constant critical diameter of 50 nm at SS=0.6%, the CCN number concentration is averagely 1.13 times of that with varied critical diameters during the NPF events. Under similar conditions, the CCN number concentration at SS=0.4% with a constant critical diameter of 70 nm is 1.15 times of that with varied critical diameters. These results will be added into the MS.

Modification in the MS:

"In our case, the mean critical diameter is around 50 nm at SS=0.6%. Assuming a constant critical diameter of 50 nm at SS=0.6%, the CCN number concentration is averagely 1.13 times of that with varied critical diameters during the NPF events. Under similar conditions, the CCN number concentration at SS=0.4% with a constant critical diameter of 70 nm is 1.15 times of that with varied critical diameters."

****

page 8425, Table 1 Please include GR_obs for each size range.

Response:

In table 1, $F_{GRH2SO4}=GR_{H2SO4}/GR_{obs}$ is the ratio of H_2SO_4 condensational growth to the observed particle growth rate. Here, GR_{obs}s for 35, 50, and 75 nm were calculated over the time period during which mean geometric diameter of log-normal ultrafine particle mode grew to 35, 50, and 75 nm, respectively, as indicated by the white circles in the Fig.1 (a).

Modification in the MS:

One sentence is added into the MS

"Here, GR_{obs}s for 35, 50, and 75 nm were calculated over the time period during which mean geometric diameter of log-normal ultrafine particle mode grew to 35, 50, and 75 nm, respectively, as indicated by the white circles in the Fig.1 (a)."

****

page 8426, Fig. 1 There are so many parameters in this graph that it is getting difficult to read. Please

1. plot H2SO4 and N3-10 on logarithmic axis (see e.g. Sihto et al., 2006)

2. plot CS in its own panel

3. plot OA mass fraction in its own panel, or preferably prepare a new figure showing the AMS data for the study period (cf. Zhang et al., 2004)

Response:

Figures are replotted and added into the MS:

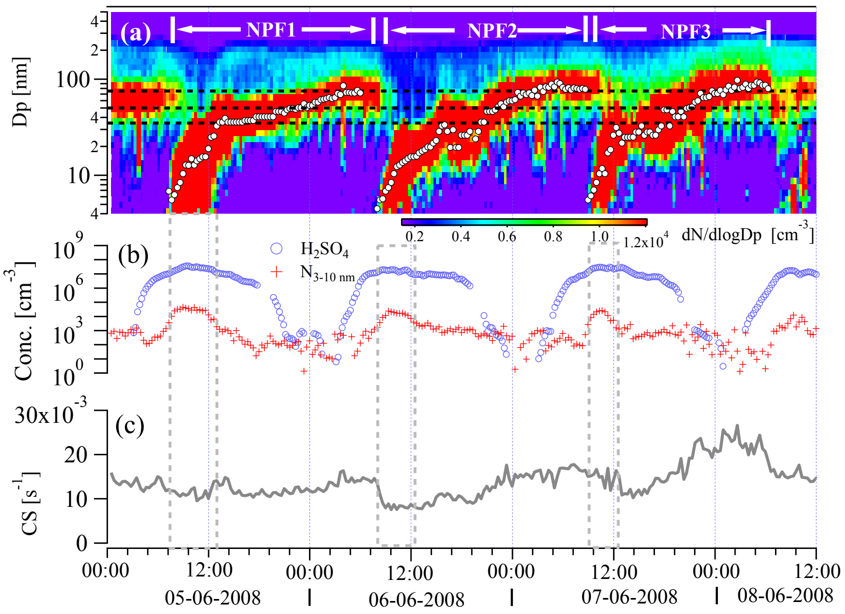

Fig. 1: Particle number size distribution (a), 3-10 nm particle number concentration and H_2SO_4 concentration (b), condensation sink (CS) (c) during the NPF events. The starting and ending time of the events were marked in the upper place of panel (a) by NPF1, NPF2, and NPF3. The while circles in the panel (a) are the D_m of new particles modes. The grey dashed lines indicated the time period of particle formation.

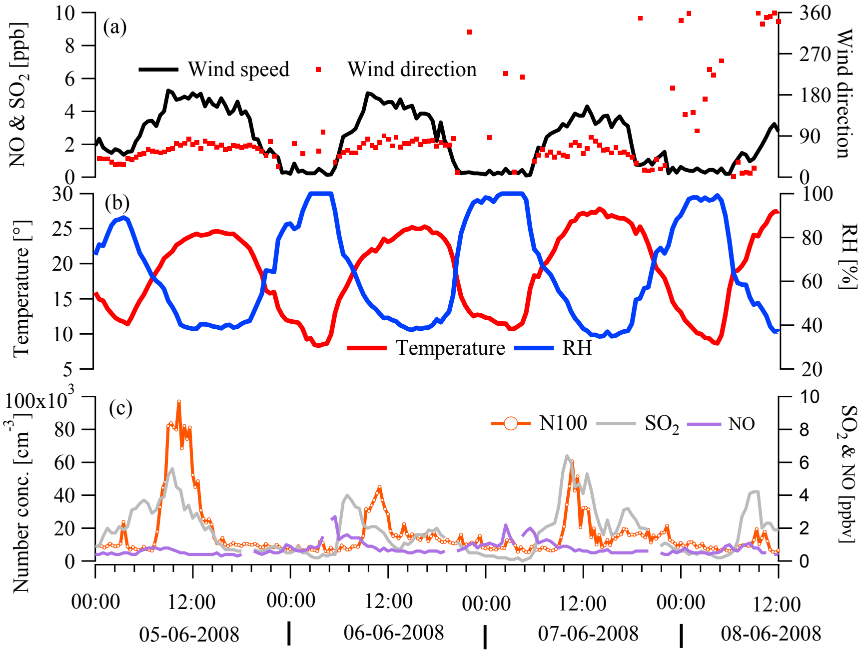

Fig. 2: The time series of wind speed and wind direction (a), ambient temperature and RH (b), and SO_2 & NO concentrations and number concentrations of particles in diameters of 3-100 nm (b).

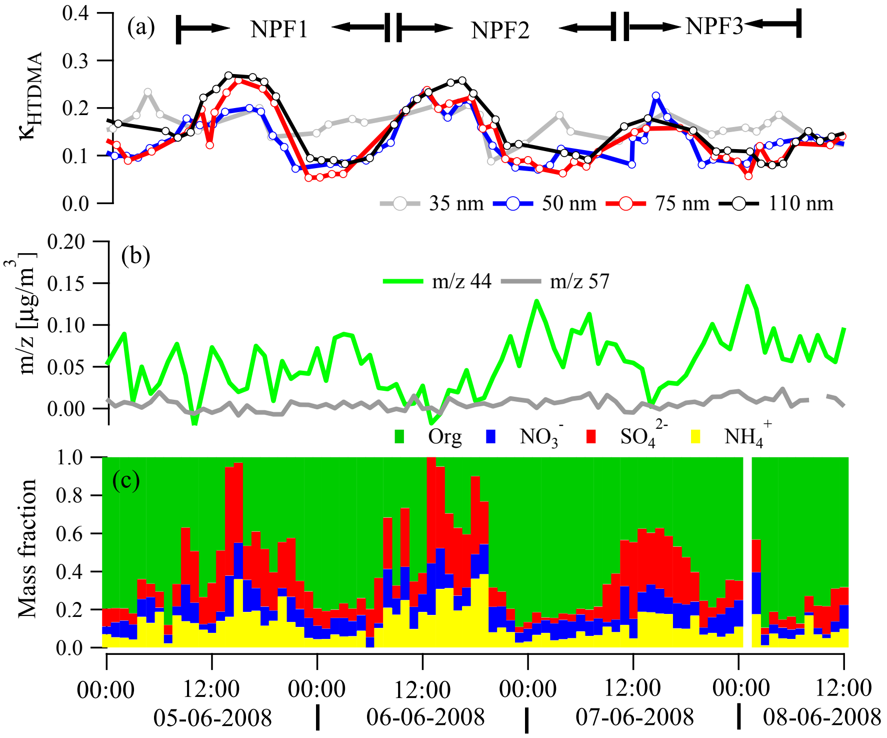

Fig.3: Size-resolved particle hygroscopicity (a), m/z 44 and 57 mass concentrations in 30-100 nm particles (b), and mass fraction of organic, sulfate, nitrate, and ammonium in 30-100 nm particles (c).

****

page 8427, Fig. 2 ss=0.1% seems to be on the right axis. Please indicate if both ss=0.4% and ss=0.6% are on the left axis.

Response:

It was corrected.

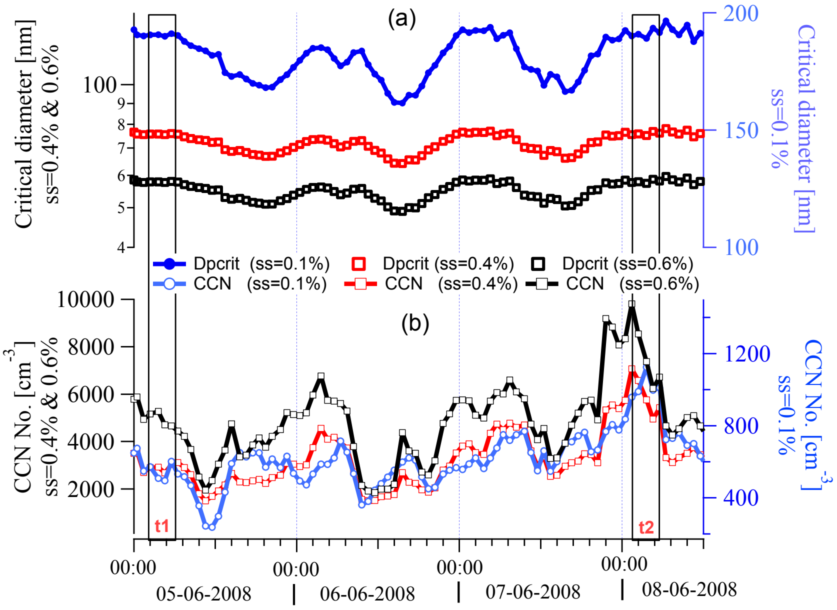

References

Canagaratna, M. R., Jayne, J. T., Jimenez, J. L., Allan, J. D., Alfarra, M. R., Zhang, Q., Onasch, T. B., Drewnick, F., Coe, H., Middlebrook, A., Delia, A., Williams, L. R., Trimborn, A. M., Northway, M. J., DeCarlo, P. F., Kolb, C. E., Davidovits, P., and Worsnop, D. R.: Chemical and microphysical characterization of ambient aerosols with the aerodyne aerosol mass spectrometer, Mass Spectrometry Reviews, 26, 185-222, 10.1002/mas.20115, 2007.

Dal Maso, M., Kulmala, M., Riipinen, I., Wagner, R., Hussein, T., Aalto, P. P., and Lehtinen, K. E.: Formation and growth of fresh atmospheric aerosols: eight years of aerosol size distribution data from SMEAR II, Hyytiala, Finland, Boreal Environment Research, 10, 323, 2005.

Heintzenberg, J.: Properties of the Log-Normal Particle Size Distribution, Aerosol Science and Technology, 21, 46-48, 10.1080/02786829408959695, 1994.

Laakso, L., Petäjä, T., Lehtinen, K. E. J., Kulmala, M., Paatero, J., Hõrrak, U., Tammet, H., and Joutsensaari, J.: Ion production rate in a boreal forest based on ion, particle and radiation measurements, Atmos. Chem. Phys., 4, 1933-1943, 10.5194/acp-4-1933-2004, 2004.

Mutzel, A., Poulain, L., Berndt, T., Iinuma, Y., Rodigast, M., Böge, O., Richters, S., Spindler, G., Sipilä, M., Jokinen, T., Kulmala, M., and Herrmann, H.: Highly Oxidized Multifunctional Organic Compounds Observed in Tropospheric Particles: A Field and Laboratory Study, Environmental Science & Technology, 49, 7754-7761, 10.1021/acs.est.5b00885, 2015.

Zhang, Q., Stanier, C. O., Canagaratna, M. R., Jayne, J. T., Worsnop, D. R., Pandis, S. N., and Jimenez, J. L.: Insights into the Chemistry of New Particle Formation and Growth Events in Pittsburgh Based on Aerosol Mass Spectrometry, Environmental Science & Technology, 38, 4797-4809, 10.1021/es035417u, 2004.

The paper presents a case study of three consecutive new particle formation events in a regional background station in Europe. Hygroscopicity measurements and AMS data are used to draw conclusions about the contributions of sulfuric acid and organic vapors to the growth of the newly formed particles to CCN sizes. CCN concentrations are calculated from size distributions and chemical composition data. The paper combines very useful measurements and calculations, but could make better use of its data and should be more rigorous in the presentation of the analyses. The following issues should be addressed before publication:

****

Thank you very much for spending a lot of time to give many good suggestions and comments. We will answer the following questions point by point.

****

Major comments:

1) No particle sources other than the NPF events seem to have been taken into consideration in the analysis. Melpitz is not a pristine environment, and even if the possible contribution of local sources can be excluded during the three-day period of observation (the paper does not state how or if this was done), wind direction can still change aerosol characteristics substantially within the time it takes for newly formed particles to grow to CCN sizes. How do the authors know that the results of their calculations pertain to aerosol particles specifically originating in the nucleation events when many hours have passed, as is the case for the calculated increases in CCN concentrations in section 4.3? How do the authors account for meteorological conditions, such as concentration/dilution due to boundary layer dynamics, when observing concentration changes (such as CCN concentrations)?

****

Response:

There are no local emission sources in the surrounding areas of the Melpitz research station. The possible primary emissions contributing to the atmospheric particles in Melpitz could be from the cities away tens of kilometers from the station via transportation. Typically, the primary particles are accompanied by trace gases, such as NO and SO_2 spikes. However, such phenomena were not observed in our measurements in Melpitz. As shown in Fig.1, in the early morning on 6 and 7 June, the slight enhancement of NO (a tracer for traffic related ultrafine particles (Janhäll et al., 2004)) concentration may be caused by the outflow of cities nearby Melpitz. We can note that the particle number concentration did not increased simultaneously. The small particles exhausted from car tailpipes in the cities may grow by condensation and coagulation and shift towards larger diameters and diluted by fresh air significantly with increasing distance from the roads (Zhu et al., 2002). As a result, the enhancement in particle number concentration was not observed in the rural site of Melpitz. Therefore, the instant impacts of primary emissions on atmospheric particles in Melpitz are not observed during the time period focused in our study. SO_2 from primary emissions contributes to the atmospheric nucleation after being oxidized to sulfuric acid by radicals. The new particle formation associating with enhanced SO_2 concentration was observed by many previous studies (e.g. Birmili and Wiedensohler, 2000).

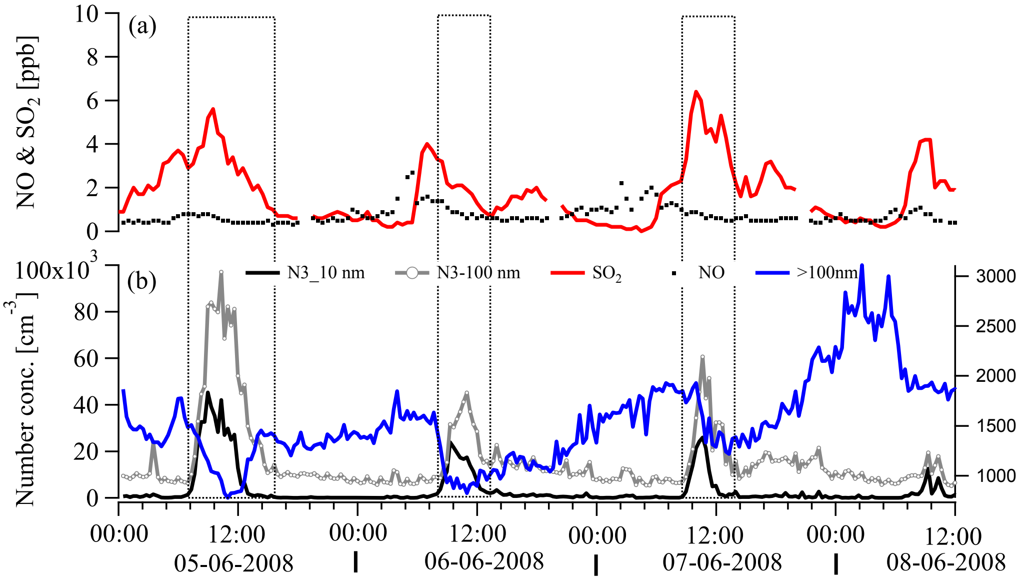

Fig. 1: The time series of SO_2 and NO concentrations (a) and number concentrations for particles in diameters of 3-10 nm, 3-100 nm, and larger than 100 nm (b).

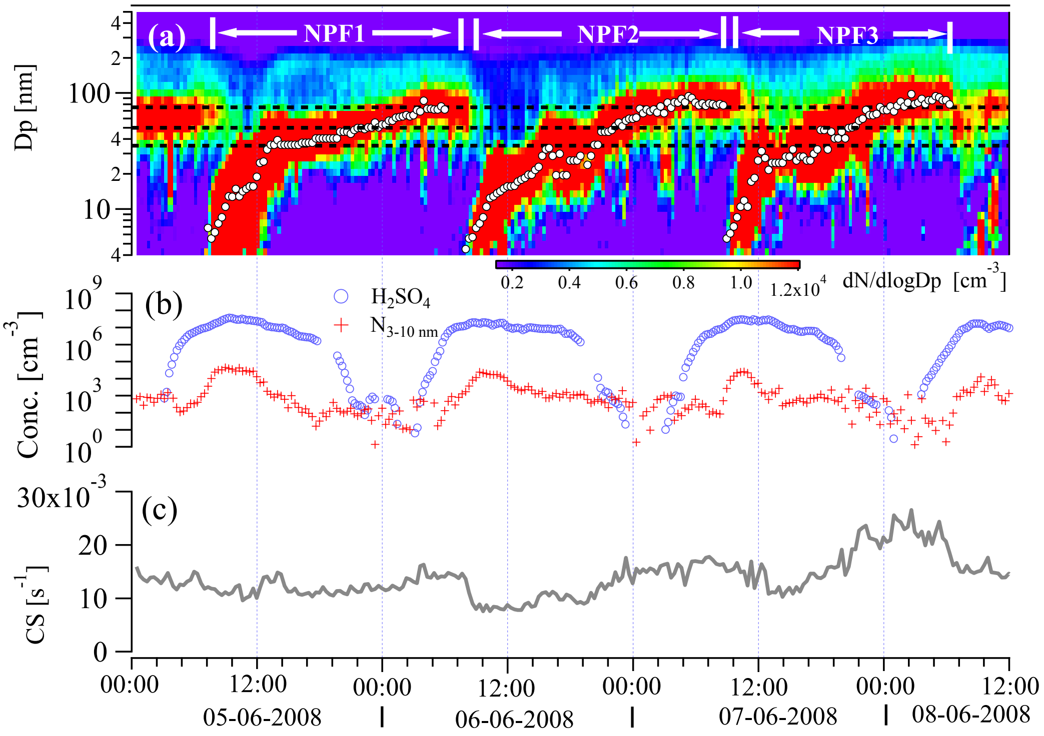

Fig. 2: Particle number size distribution, 3-10 nm particle number concentration, H_2SO_4 concentration, condensation sink (CS) during the new particle formation events.

From the regional scale point of view, the primary particles, such as soot particles are diluted after emission and gradually change into uninform distribution in the air with increasing distance from the emission sources. The lifetime of fine particles is around 1 week. The time period is 3 days. The primary particles could accumulate in the air and increase the CCN number. However, compared to the particle concentration contributed by nucleation and growth, the contribution of primary particles to CCN number can be ignored.

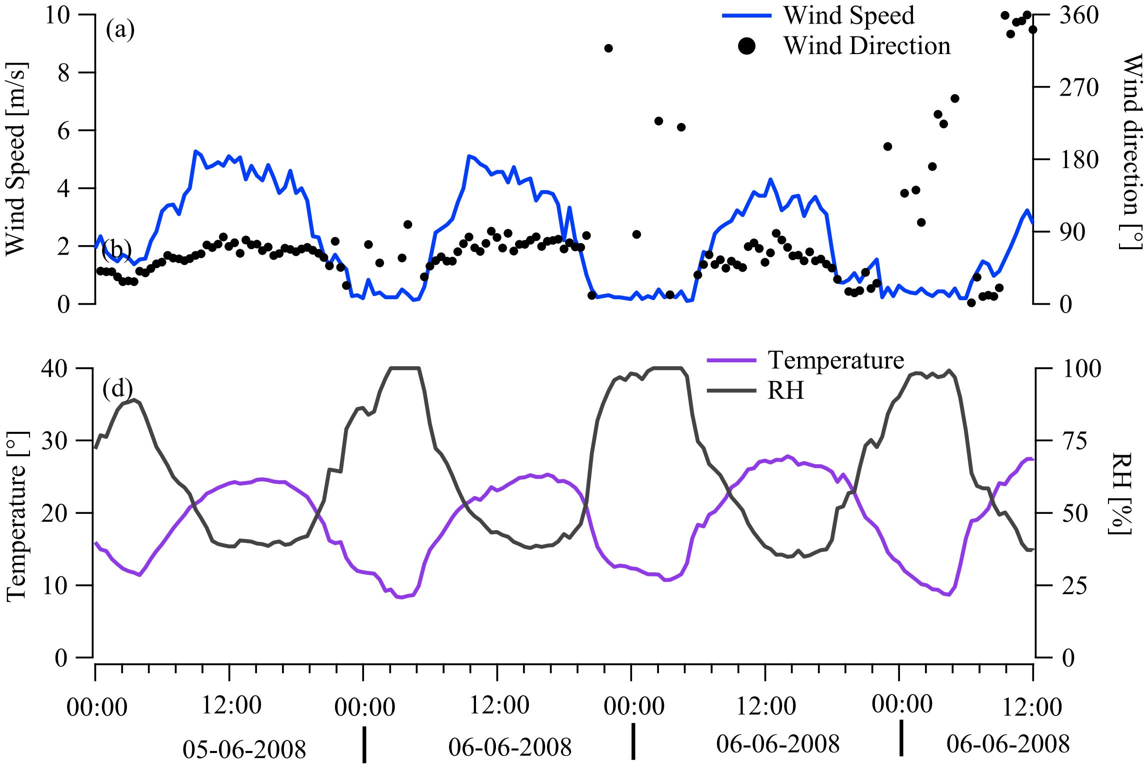

Fig. 3: The time series of wind speed, wind direction, ambient temperature, and RH during the NPF events.

As displayed in Fig.2, the particle number size distribution shows the new particle formed around 10 am and then grew versus time for more than 20 h. This shows that the NPF is a regional event (refere to Hussein et al., 2000) and could take place over a distance of a hundred kilometers. The Fig.3 shows the wind speed and wind direction during the NPF events. The wind showed a typical diurnal cycle. The wind speed is 4-5 m/s and kept a constant direction (south) during daytime. It is static wind during nighttime. No sharp change in wind direction and wind speed were observed.

Atmospheric boundary layer development and turbulent mixing will impact on NPF (Boy et al., 2006;Boy et al., 2003;Altstädter et al., 2015), and consequently on its CCN products. It is hard task to quantify the changes in CCN number due to boundary layer dynamics. In this study, the enhancement in CCN number concentration caused by atmospheric nucleation was evaluated by comparing the average CCN number concentrations over two hours prior to the beginning of the event (the period t1 marked in Fig. 4) with the same time period before the end of the events (the period t2 marked in Fig. 4). The weather conditions (see RH and T in Fig. 3) are quite similar during the three NPF days. Here we assume that the weather condition and boundary layer height are similar during two time periods. In addition, the enhancement factor of CCN number concentration is a ratio of CCN concentration during two periods and not an absolute value. To some extent, the ratio can weaken the influence of boundary layer dynamics. In addition, the ratio can exclude the effect of primary emission on CCN number. This is because that the contribution of primary particles to CCN number should be similar at the same time period on different days.

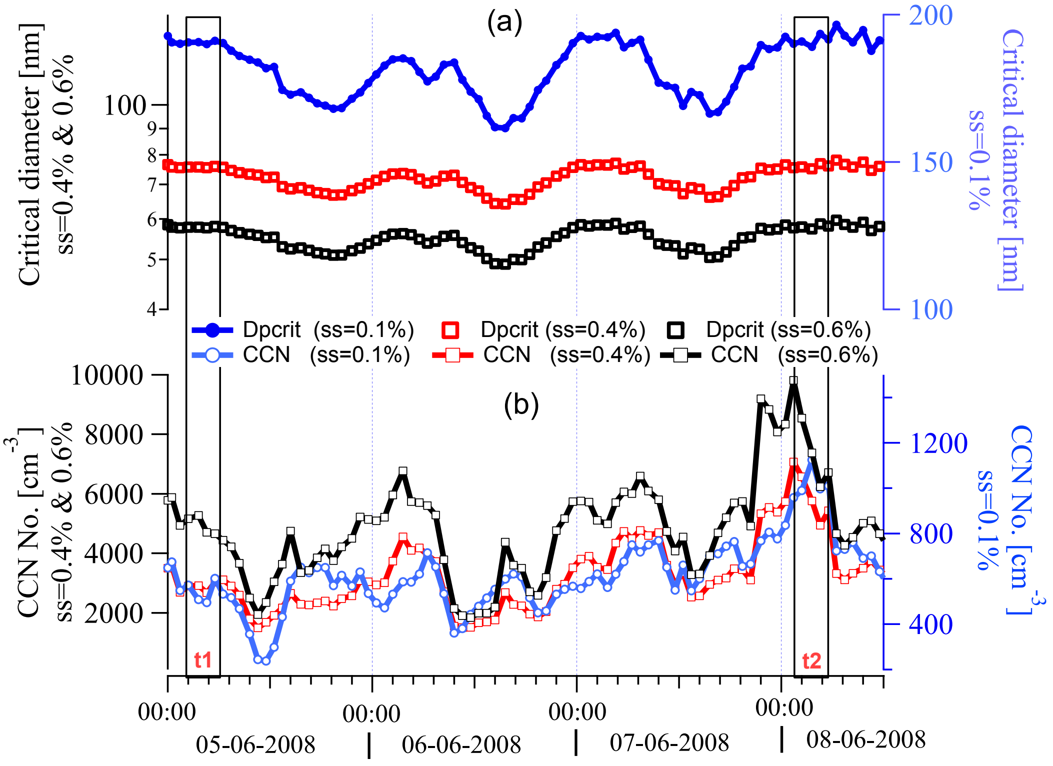

Fig.4: Critical diameter and CCN number concentration during NPF events.

According to the above-analysis, we can see that the new particle formation and growth is a major particle source at Melpitz. The NPF at a regional scale makes more meaningful for contributing the CCN number. The increased nucleation mode particle number concentration was followed with sulfuric acid concentration. This confirms that the particles mainly originated from atmospheric nucleation and subsequent growth, not from the primary emissions.

Modification in the MS

Modification in section “4.1 Particle formation and growth”

“The previous study on the basis of long-term observations showed that the NPF events take place frequently at Melpitz, especially on April, May, and June (Hamed et al., 2010). In present study, three NPF events, which consecutively took place from June 5 to June 7, 2008, as displayed in Fig. 1 (a), are selected for further analysis. These events are the best cases which showed clear particle bursts and subsequent growth process during the entire field campaign (from May 23rd to June 8th in 2008). The starting and ending time for each event were marked in the Fig.1 (a) as NPF1, NPF2, and NPF3. The bursts in number concentration of 3-10 nm particles were observed associated with increasing ambient temperature, decreasing relative humidity (shown in Fig. 2 (b)), and increasing in estimated H_2SO_4 concentration (shown in Fig. 1(b)). The condensation sink (CS) is between 0.01 and 0.02 s^{-1} during the NPF events. As marked in Fig.1 (a), the particle number size distribution shows the new particle formed around 10 am and then grew versus time for more than 20 h. This means that the NPF is a regional event (refere to Hussein et al., 2000) and could take place over a distance of a hundred kilometers. The Fig.2 (a) displays the wind speed and wind direction during the NPF events. The wind showed a typical diurnal cycle. The wind speed is 4-5 m/s and kept a constant direction (south) during daytime. It is static wind during nighttime. The particle formation rates ($J_{3\text{-}25nm}$) were 13.5, 6.1, 9.3 $cm^{-3}s^{-1}$ on June 5, 6, and 7, respectively. The highest formation rate was observed on June 5 corresponding to the highest H_2SO_4 concentration.

As indicated by the white circle in the Fig.1 (a), the mean geometric diameter (Dm) of log-normal ultrafine particle mode increased to around 100 nm within 24 hours. Over the time period from the beginning to the end of the NPF events as marked in Fig.1 (a), the average GR_{obs}s were respectively 2.8, 3.6, and 4.4 nm h^{-1} for NPF events on June 5th, 6th, and 7th, 2008. One can note that the new particles continued growing during nighttime when sulfuric acid concentration was close to zero. This indicated that other species, most likely, organic compounds contributed to the particle growth during this time period.

There are no local emission sources in the surrounding areas of the Melpitz research station. The possible primary emissions contributing to the atmospheric particles in Melpitz could be from the cities away tens of kilometers from the station via transportation. Typically, the primary particles are accompanied by trace gases, such as NO and SO_2 spikes. However, such phenomena were not observed in our measurements at Melpitz. As shown in Fig.2 (c), in the early morning on 6 and 7 June, the slight enhancement of NO (a tracer for traffic related ultrafine particles (Janhäll et al., 2004)) concentration may be caused by the outflow of cities nearby Melpitz. The particle number concentration did not increased simultaneously. The ultrafine particles exhausted from car tailpipes in the cities may grow by condensation and coagulation and shift towards larger diameters and diluted by fresh air significantly with increasing distance from the roads (Zhu et al., 2002). As a result, the enhancement in ultrafine particle number concentration was not observed at the rural site of Melpitz. Therefore, the instant impacts of primary emissions on atmospheric particles are not observed during the time period focused in this study. SO_2 from primary emissions could contribute to the atmospheric nucleation after being oxidized to sulfuric acid by radicals. The new particle formation associating with enhanced SO_2 concentration was observed by many previous studies (e.g. Birmili and

Wiedensohler, 2000). Overall, the new particle formation and subsequent growth is the major source of particles, and thereby, CCN at Melpitz station. ”

****

2) It seems to me that the available data should be exploited better. For example, size-resolved AMS data are available, but, as far as I can tell, are only made use of in the calculation of D(crit). In describing changes in the organic fraction during the NPF events, instead of using PM1, the size-resolved AMS data could be used to more accurately represent chemical composition of the smaller particle size range, thereby reducing the potential dominance of large particles (possibly from sources other than NPF) in the mass concentrations. Also, with those size-resolved AMS data available, why is all hygroscopicity and all condensational growth reduced to sulfate and organics? With HTDMA data available, it may be possible to derive a kappa (HTDMA), and use that for the calculation of the expected CCN concentrations – was there a specific reason the authors decided to use only the AMS chemistry + size distribution data?

****

Response:

Considering the accuracy of size-resolved particle mass concentration detected by AMS and the transmission efficiency of aerodynamic lenses (Canagaratna et al., 2007), the chemical composition of 30-100 nm particles is chosen to perform the analysis. Some discussions were added into the manuscript.

The HTDMA-derived kappa was not used in calculating the critical diameter. This reason is given as follow: The inconsistencies between HTDMA-derived kappa and CCNc-derived kapp have been reported in several previous studies (Good et al., 2010;Cerully et al., 2011;Irwin et al., 2010;Petters et al., 2009;Wex et al., 2009). Possible explanations are non-ideality effects in the solution droplet, surface tension reduction due to surface active substances, and the presence of slightly soluble substances which dissolve at RHs larger than the one considered in the H-TDMA (Wex et al., 2009). Due to these effects, is not necessarily constant and may vary with humidity. Extrapolating from HTDMA data to properties at the point of activation should be done with great care. In addition, the previous studies showed that critical diameters at different supersaturations can be well-predicted using AMS data and ZSR method. Therefore, the AMS data was decided to use to estimate the critical diameters instead of HTDMA-derived kappa.

Modification in the MS

As displayed in Fig.3 (c), the sulfate and ammonium were dominated in the inorganic mass fraction in 30-100 nm particles and obviously increased during the particle formation period (indicated by grey dashed line in Fig.1). While, the nitrate accounted for a minor fraction, which also observed by Zhang et al. in Pittsburgh (Zhang et al., 2004). They found nitrate contributed the least to the new particle growth. After 3:00pm on each day, the organic mass fraction increased and reached its maximum at midnight, indicating that organics played a key role in the particle growth at a relatively later time of the NPF event. The mass fraction of ion fragments m/z 44 and 57 in 30-100 nm particles are shown in the Fig. 3(b). The m/z 44 (CO_2^+ ion fragment) is a tracer for secondary organic aerosol，while m/z 57 ($C_4H_9^+$) is generally associated with primary organics from combustion sources (Zhang et al., 2004). The m/z 57 mass concentration is close to zero during the events. Compared m/z 57, the m/z 44 mass concentration are considerable, indicating that the organics contributing to particle growth was mainly secondary organic species.

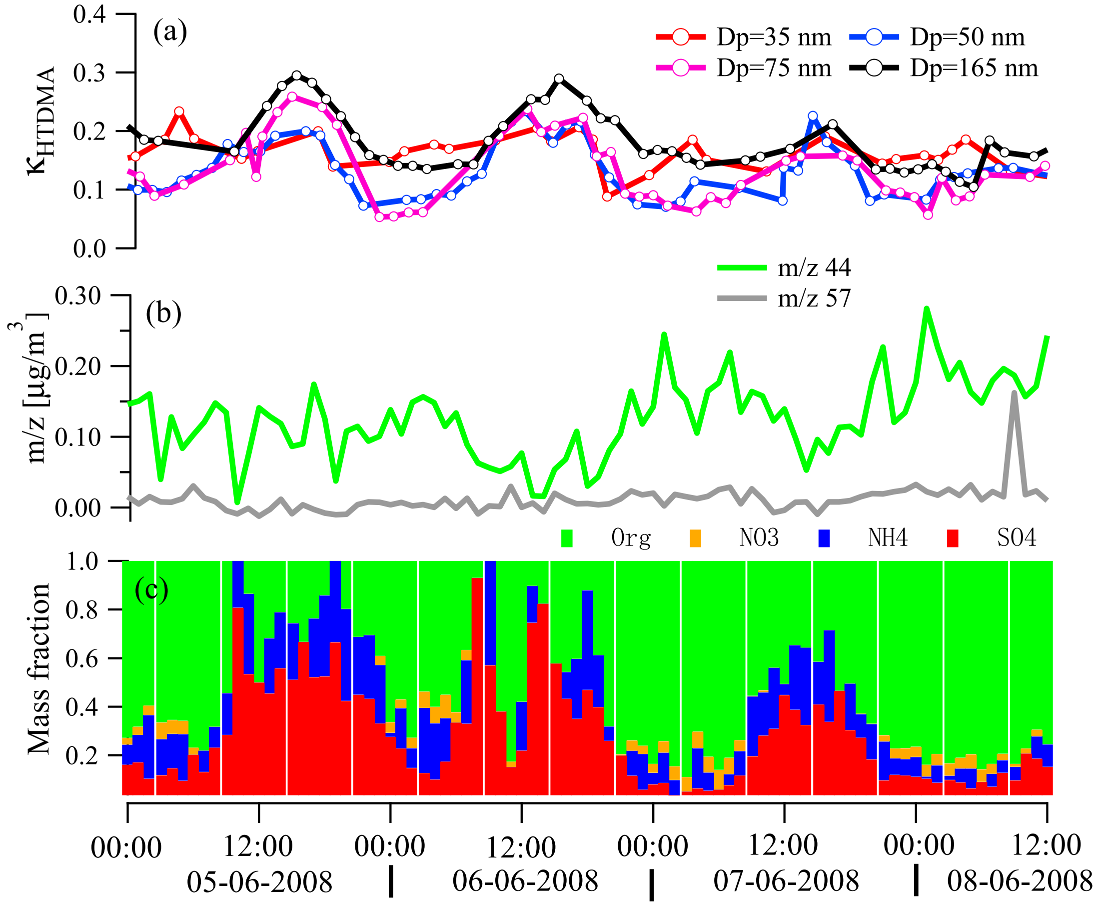

Fig.3: Size-resolved particle hygroscopicity and mass fraction of particle below 150 nm in mobility diameter.

Some texts were added into the section 3.2

“The HTDMA-derived κ was not used in calculating the critical diameter. This reason is given as follow: The inconsistencies between HTDMA-derived kappa and CCNc-derived κ have been reported in several previous studies (Good et al., 2010;Cerully et al., 2011;Irwin et al., 2010;Petters et al., 2009;Wex et al., 2009). Possible explanations are non-ideality effects in the solution droplet, surface tension reduction due to surface active substances, and the presence of slightly soluble substances which dissolve at RHs larger than the one considered in the H-TDMA (Wex et al., 2009). Due to these effects, κ is not necessarily constant and may vary with humidity. Extrapolating from HTDMA data to properties at the point of activation should be done with great care (Wu et al., 2013). In addition, the our previous study (Wu et al., 2013) showed that critical diameters at different supersaturations can be well-predicted using AMS data and ZSR method. Therefore, the AMS data was decided to use to estimate the critical diameters instead of HTDMA-derived κ. ”

****

3) There is important information missing, such as: What were the kappa(i) values used that entered the kappa(chem) calculation? How and over what time period was GR(obs) calculated? How were the hygroscopic growth factors derived from the HTDMA data? The description of the results is also missing information: Increases/decreases are described without giving the time period over which increases/decreases were observed, or how large the increases/decreases were. How are the beginning, end, and duration of an NPF event defined? When stating that something was observed "during the events", what exact time frame does that refer to? Also, for which exact points during the particle growth were the soluble fractions calculated?

****

Response:

The information on the input parameters in the calculation will be added in the manuscript. The starting and ending time of PNF events were marked in the Fig. 1 (a).

Modification in the MS

In section 3.2:

“We use a simplified ion pairing scheme as presented in Gysel et al. (2007) to convert the ion mass concentrations to the mass concentrations of their corresponding inorganic salts as listed in Table 2.”

Table 2: Gravimetric densities and hygroscopicity parameters κ used in this study.

Species	**NH_4NO_3**	**H_2SO_4**	**NH_4HSO_4**	**$(NH_4)_2SO_4$**	**Organic matter**
[kg/m^3]	1720	1830	1780	1769	1400
	0.67	0.92	0.61	0.61	0.1

In section 4.1:

“The previous study on the basis of long-term observations showed that the NPF events take place frequently at Melpitz, especially on April, May, and June (Hamed et al., 2010). In present study, three NPF events, which consecutively took place from June 5 to June 7, 2008, as displayed in Fig. 1 (a), are selected for further analysis. These events are the best cases which showed clear particle bursts and subsequent growth process during the entire field campaign. The starting and ending time for each event were marked in the Fig.1 (a) as NPF1, NPF2, and NPF3."

"Over the time period from the beginning to the end of the NPF events as marked in Fig.1 (a), the average GR_{obs}s were respectively 2.8, 3.6, and 4.4 nm h^{-1} for NPF events on June 5th, 6th, and 7th, 2008."

****

Comments on the writing:

1) There are multiple language errors, which should be corrected (singular/plural errors, missing/superfluous articles, wrong punctuations), as they can hamper the understanding of the material, e.g.: p. 8405, line 26 "sulfuric acid and organics, which fraction is the leading component in particles: : :", p.8406, line "measurements during a NPF events", p. 8406: "in the polluted areas, Atlanta, USA", p. 8413 "took place from, 5 to 7 June 2008, ".

Response:

These errors were corrected in the MS.

2) There are many references in the text that are missing in the list of references, e.g. p. 8408, lines 21-23.

Response:

The MS was checked very carefully. The missing references were added in the MS.

****

Specific comments by section:

Introduction:

p. 8405, line 8: "the single largest uncertainty" of what? In the statement by Kerminen et al. that is most likely cited here, nucleation is not stated to be "the single largest uncertainty" in the CCN budget.

Response:

"the single largest uncertainty" was modified to "The contribution of atmospheric nucleation to the global CCN budget spans a relatively large uncertainty range".

p. 8405, line 9: "radioactive" should be "radiative"

Response:

It was corrected in the MS.

p. 8406, line 6: what are "potential chemical species"?

Response:

"Potential" is removed from the texts.

****

Experiments:

Perhaps the title “Measurements”, or “Experimental” would be better, as “Experiments” could raise the expectation of a controlled laboratory setup.

Response:

We agree. The “Measurements” was used instead of “Experiments”

p. 8406, line 15: Could the authors provide a little more information on the full dataset that this case study is a part of, and specifically, state why were those exact three days chosen? How many events were observed in the full dataset? Please also describe the origin of SO2 and Rad, used later in this study.

Response:

The particle number size distribution, gaseous pollutants, and meteorological parameters are routinely measured at Melpitz research station. The HR-Tof-AMS was operated only during the intensive field campaign from May 23rd to June 8th, 2008. The following table summarizes all instruments and measured parameters used in this study.

The previous study on the basis of long-term observations showed that the NPF events take place frequently at Melpitz, especially on April, May, and June (Hamed et al., 2010). In present study, three NPF events selected are the best cases which showed clear particle bursts and subsequent growth process during the time period with available AMS and HTDMA data. These NPF events are typical regional event, which spanned a larger spatial scale and therefore more significant impacts on CCN number concentration at a regional scale.

Modification in the MS

One table was added into the “Measurements” section and summarizes the instruments and parameters used in this manuscript.

Table: The summary of instrument and parameters used in this study

Instrument	Parameter
SMPS	Particle number size distribution
HTDMA	Particle hygroscopicity
HR-ToF-AMS	Size-resolved chemical composition
Monitor – APSA 360 Horiba Europe	SO_2 concentration
Kipp & Zonen CM6 Pyranometer	Global solar irradiance

An explanation was added into the manuscript to explain why only three events were selected in this study.

“The previous study on the basis of long-term observations showed that the NPF events take place frequently at Melpitz, especially on April, May, and June (Hamed et al., 2010). In present study, three NPF events, which consecutively took place from

June 5 to June 7, 2008, as displayed in Fig. 1 (a), are selected for further analysis. These cases are the typical regional events which showed clear particle bursts and subsequent growth process during the time period with available AMS and HTDMA data.”

****

Section 2.1:

The HTDMA measurements should be described better: which dry sizes and RH’s were chosen? What was the sampling schedule for the chosen parameters? How were the growth factors determined from the size distribution of DMA2?

Response:

The particles with dry sizes of 35, 50, 75, 110, 165, and 265 nm were measured by HTDMA at RH=90% with time resolution of 1 h. In this study, the HGFs of 35, 50, and 75 nm particles are used only. The HTDMA raw data were inverted using the TDMAinv method developed by Gysel et al. (2009). In Gysel’s article, the TDMAinv method is introduced very detailed. Here, we will not give unnecessary details.

Modification in the MS

One sentence was added into the MS.

“In this study, the particles with dry sizes of 35, 50, 75, 110, 165, and 265 nm were measured by HTDMA at RH=90% with the time resolution of 1h. The HGFs of 35, 50, and 75 nm particles will be taken for further analysis. ”

p. 8407, line 2: “described” is better than “illustrated”

Response:

It was changed in the texts.

****

Section 2.2:

Please provide a lower particle size detection limit of the AMS.

Response:

The aerodynamic lenses have 100% transmission efficiency down to 70 nm in a vacuum aerodynamic diameter (Canagaratna et al., 2007).

Modification in the MS:

One sentence was added into the MS: “The aerodynamic lenses have 100% transmission efficiency down to 70 nm in a vacuum aerodynamic diameter (Canagaratna et al., 2007).”

p. 8407, line 24: “typically”: Since the investigated dataset is only three days, could the authors give more detail here?

Response:

The “typically” was removed from the texts.

p. 8408, line 8: How was the density value chosen?

Response:

We estimated the gravimetric particle density on the basis of measured chemical composition using the following equation:

$$\text{density} = \frac{[\text{Total}_{\text{AMS}} + \text{BC}]}{\frac{[\text{NO}_3^-]+\left[\text{SO}_4^{2-}\right]+[\text{NH}_4^-]}{1.75} + \frac{[\text{Cl}-]}{1.52} + \frac{[\text{Org}]}{1.2} + \frac{[\text{BC}]}{1.77}}$$

The mean particle density is 1.4 g cm^{-3} for May–June 2008. The detail description was given in (Poulain et al., 2014)

Modification in the MS:

"The particle density was calculated on the basis of measured chemical composition. The detail description about the calculation was given in Poulain et al. (2014)."

p. 8409, line 3: "two groups including soluble and insoluble fractions" – this is confusing. How many groups or fractions were there?

Response:

This sentence was rewritten in the texts.

"Here, the chemical compounds contributing to the particle growth are grouped into two fractions, e.g., soluble and insoluble fractions."

p. 8409, line 13 and following: Should the assumption of an insoluble organic fraction not underestimate the actual soluble fraction of the particle?

Response:

Yes, we agree. The assumption of an insoluble organic fraction may lead to overestimate the soluble fraction.

p. 8409, line 17: It would be helpful if the term "equivalent soluble fraction" was used consistently from this point onward.

Response:

The term "equivalent soluble fraction" was used consistently in the texts.

****

Section 3.2:

p. 8410, line 9: The size ranges of the AMS measurements, the chemical species used in the calculation, as well as the values used for their respective kappa(i) should be stated here.

Response:

A detail description is given in the manuscript.

Modifications in the texts:

“The AMS provides the particle mass size distribution of sulfate (SO_4^{2-}), nitrate (NO_3), and ammonium (NH_4^+) ions as well that of organic compounds. We use a simplified ion pairing scheme as presented in Gysel et al. (2007) to convert the ion mass concentrations to the mass concentrations of their corresponding inorganic salts as listed in Table 2.”

Table 2: Gravimetric densities ρ and hygroscopicity parameters κ used in this study.

Species	NH_4NO_3	H_2SO_4	NH_4HSO_4	$(NH_4)_2SO_4$	Organic matter
ρ [kg/m^3]	1720	1830	1780	1769	1400
	0.67	0.92	0.61	0.61	0.1

p. 8410, line 15: “are activated”, not “were activated” p. 8410, line 16: Please state which critical supersaturations were chosen for the calculation.

Response:

It was corrected in the text:

“DPcrit is the critical diameter at which 50% of the particles were activated at the supersaturation, Sc (0.1%, 0.4%, and 0.6 are chosen).”

p. 8410, line 19: Integrating the size distribution from D(crit) upwards: The implicit assumption of an internal mixture of the determined (bulk) chemical composition should be stated explicitly here.

Response:

The sentence “The CCN number concentration is estimated by integrating the particle number size distribution from the critical diameter to the maximum diameter detected by TDMPS (800 nm, above which the particle number concentration is generally negligible), assuming particles are internal mixture.” was added into the texts.

p. 8410, line 22 and following: This discussion is confusing in its current location in the section: “The critical diameters” (p. 8411, line 1) could be interpreted as the critical diameters in this study, calculated from eq. 5, rather than a general statement on the approximate range of critical diameters, which, I believe, is what the authors mean. This description of the chosen AMS size ranges should be moved up, as stated in the initial comment on this section.

Response:

The texts in line 22 and following of p.8410 were moved up to the initial part of this section.

Modification in the MS:

“The CCN number concentration can be estimated by integrating the particle number size distribution from the critical diameter to the maximum diameter detected by

TDMPS (800 nm, above which the particle number concentration is generally negligible), assuming particles are internal mixture. The critical diameter (D_{pcrit}) at which 50% of the particles are activated is calculated from κ:

$$D_{Pcrit} = \left(\frac{4A^3}{27\,\kappa_{chem}\ln^2 S_C}\right)^{1/3} \quad [6]$$

Here, κ_{chem} is calculated from size-resolved AMS data using the ZSR mixing rule. D_{Pcrit} is the critical diameter at which 50% of the particles were activated at the supersaturation, S_c (0.1%, 0.4%, and 0.6% are chosen in this study).
According to the κ-Köhler theory (Petters and Kreidenweis, 2007), the single hygroscopicity parameter, κ, of a given internal mixture can be predicted by a mixing rule on the basis of chemical volume fractions ε_i:

$$\kappa_{chem} = \sum_i \varepsilon_i \kappa_i \quad [7]$$

Here, κ_i and ε_i are the hygroscopicity parameter and volume fraction for the individual (dry) component in the mixture with *i* the number of components in the mixture. We derive ε_i from particle chemical composition measured by AMS. Here, the size-resolved particle chemical composition is used to estimate the κ_{chem}. The size-resolved chemical composition was used to calculate the κ values. The critical diameters, corresponding to supersaturation 0.2-0.7%, roughly span from 50 to 120 nm in mobility diameter. Therefore, the chemical composition of 50-120 nm particles was calculated by integrating AMS mass size distribution data and used to estimate κ_{chem}. In the same way, the chemical composition of 150-200 nm particles is used to calculate κ_{chem} for the critical diameter of around 170 nm, which corresponds to a supersaturation of 0.1%. The AMS provides the particle mass size distribution of sulfate (SO_4^{2-}), nitrate (NO_3), and ammonium (NH_4^+) ions as well that of organic compounds. We use a simplified ion pairing scheme as presented in Gysel et al. (2007) to convert the ion mass concentrations to the mass concentrations of their corresponding inorganic salts as listed in Table 2."

****

Section 3.4:

What were the time frames (and particle diameter ranges) that were actually used for the determination of the growth rates in this study?

Response:

The growth rate is calculated as follow:

The observed particle growth rate (GR) can be expressed as:

$$GR = \frac{\Delta D_m}{\Delta t}$$

where Dm is a mean geometric diameter of log-normal ultrafine particle mode, which has been fitted to the number size distribution (Heintzenberg, 1994). GR means evolution of the mean diameter within a time period Δt.

In the Fig.1 (a), the Dm of ultrafine particle mode is indicated as the white circles. The time frames during which GRs were calculated is from the starting and ending time marked in the Fig.1 (a).

Modifications in the texts:

More texts were added into the texts to make the calculation of growth rate clear.

"The starting and ending time was marked in the Fig.1 (a)."

"As indicated by the white circle in the Fig.1 (a), the mean geometric diameter (Dm) of log-normal ultrafine particle mode increased to around 100 nm within 24 hours. Over the time period from the beginning to the end of the NPF events as marked in Fig.1 (a), the average GR_{obs}s were respectively 2.8, 3.6, and 4.4 nm h^{-1} for NPF events on June 5th, 6th, and 7th, 2008."

p. 8412, line 19: Weren't the H2SO4 concentrations calculated, rather than measured?

Response:

The H_2SO_4 concentration is calculated. The error was corrected in the texts.

Results:

p. 8413, line 9: How was the particle formation rate calculated?

p. 8413, line 18: average over what? What was the time frame of the GR determination?

It would be helpful is "GR(obs)" were used consistently.

p. 8413, line 20: define "particle formation period"

Response:

These three questions relating to the calculation of particle formation and growth rate will be answered together. To clarify the calculation methods, one section has been added into the MS to introduce the methods for calculating the formation rate and growth rate. The starting and ending time of NPF events were marked in the Fig. 1. The growth rate is calculated within the time frame between the starting and ending points as marked in the Fig.1. The formation period is defined as the time period during which an obvious increase in the number concentration of 3-10 nm particles was observed. The formation period is marked in the Fig.1.

Modifications in the MS:

"3.4 Calculation of particle formation and growth rate

"Assuming a constant particle source during a time period of t, the particle formation rate (Jnuc) can be expressed as (Dal Maso et al., 2005):

$$J_{nuc} = \frac{dN_{nuc}}{dt} + F_{coag} + F_{growth} \qquad [10]$$

In this study, N_{nuc} is the number concentration of nucleation mode particles ranging from 3 nm to 25 nm. F_{growth} is the flux of particles out of the specified size range (3-25 nm). The newly formed particles rarely grew beyond 25 nm before formation ended, and F_{growth} can be neglected. F_{coag} represents a loss of formed particles due to coagulation to the preexisting particle population. It can be calculated from the following equation:

$$F_{coag} = CoagS_{nuc}N_{nuc} \qquad [11]$$

where $CoagS_{nuc}$ is the coagulation sink of particles in the nucleation mode. The detailed calculation of coagulation sink is given in Deal Maso et al. (2005).
The observed particle growth rate (GR_{obs}) can be expressed as:

$$GR_{obs} = \frac{\Delta D_m}{\Delta t} \qquad [12]$$

where Dm is a mean geometric diameter of log-normal ultrafine particle mode, which has been fitted to the number size distribution (Heintzenberg, 1994). GR_{obs} means evolution of the mean diameter within a time period Δt."

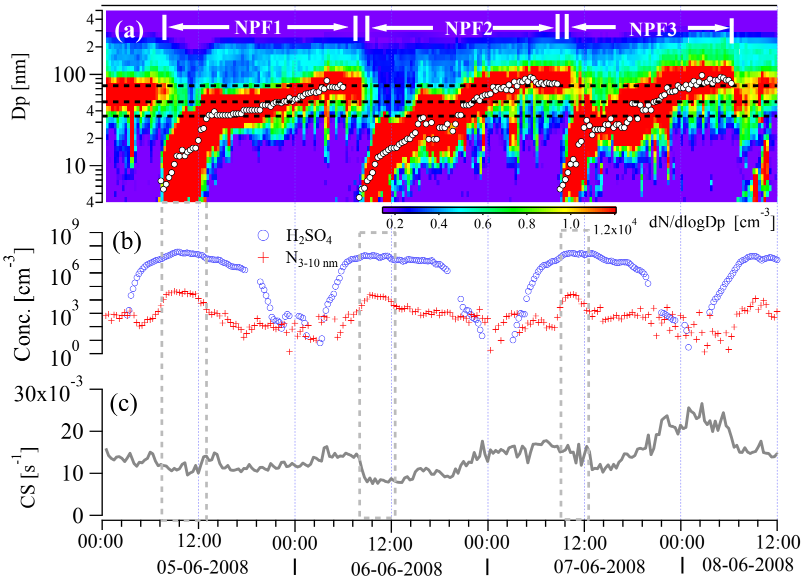

Fig. 1: Particle number size distribution, 3-10 nm particle number concentration, H_2SO_4 concentration, condensation sink (CS) during the NPF events. The starting and ending time of the events were marked in the upper place of panel (a) by NPF1, NPF2, and NPF3. The grey dashed lines indicated the time period of particle formation.

p. 8413, line 21: "This was because...": Has causality been established?

Response:

"This was because..." was removed. This sentence was rewritten.

p. 8413, line 23: "hygroscopic" would be better than "water-soluble"

Response:

"Hygroscopic" is used in the MS.

p. 8414, line 2: The processes were not observed directly. Rather, they can be inferred (to a degree) by the measurements. This should be made clear.

Response:

More texts were added into the MS

Modification in the MS:

"As shown in the Fig. 3(a), peak daily κs of 50, 75, and 110 nm particles occurred afternoon and minimum appeared in the midnight. The evolution of particle hygroscopicity was very similar to those of inorganic mass fraction (sulfate+nitrate+ammonium) in 30-100 nm particles. During the daytime, H_2SO_4 concentration increased and may condense onto the particles. At the same time, the increasing ambient temperature (see Fig. 2 (b)) could drive the semi-volatile organic species in particle phase to partition to gas phase. Both processes could result in an increasing of inorganic fraction in particle phase, thereby enhancement in particle hygroscopicity."

p. 8414, line 4: "Significant" should only be used when statistical significance is established.

Response:

"Significant" was removed from the texts.

p. 8414, line 6: Please substantiate the statement: "sulfuric acid condensation played a minor role in particle growth"? And what is the time period?

Response:

"sulfuric acid condensation played a minor role in particle growth" was removed from the texts.

p. 8414, lines 6 – 10: "Lower temperature facilitates [: : :] leading to an evident decline of hygroscopicity." It seems to me that the initial observation was the decrease in hygroscopicity and the increase in organic mass fraction, and the condensation of semivolatile compounds is a possible reason, rather than the reverse: stating a plausible process (condensation of semi-volatiles) and treating the observations as "confirming" it.

Response:

The sentences were rearranged.

Modification in the texts:

"Fig.3 displayed the size-resolved particle hygroscopicity (a), m/z 44 and 57 concentrations (b), and mass fraction of organic, sulfate, nitrate, and ammonium in 30-100 nm (mobility diameter) particles (c). As shown in the Fig. 3(a), peak daily κs of 50, 75, and 110 nm particles occurred afternoon and minimum appeared in the midnight. The evolution of particle hygroscopicity was very similar to those of inorganic mass fraction (sulfate+nitrate+ammonium) in 30-100 nm particles. During the daytime, H_2SO_4 concentration increased and may condense onto the particles. At the same time, the increasing ambient temperature (see Fig. 2 (b)) could drive the semi-volatile organic species in particle phase to partition to gas phase. Both processes could result in an increasing of inorganic fraction in particle phase, thereby enhancement in particle hygroscopicity. The decline in particle hygroscopicity took place after 15:30 (Local time) when sulfuric acid concentration decreased significantly. Simultaneously, ambient temperature decreased to 10˚C. Lower temperature facilitates the condensation of semi-volatile organic vapors onto the particles. As a result, the organic mass fraction increased significantly during nighttime, as shown by AMS measurements (Fig.3 (c)), leading to an evident decline in particle hygroscopicity.”

p. 8414, lines 9 and following: “when these particles grew to: : :” How were the hygroscopicity measurements at the different particle sizes attributed to the newly formed (rather than pre-existing) particles? How was the growth traced, and which exact hygroscopicity measurements were taken at which point in the growth process?

Response:

The equivalent water-soluble fraction 35, 50, and 75 nm particles are corresponding to the HTDMA measurement points at which the mean geometric diameter (Dm) of ultrafine particle mode reached 35, 50, and 75 nm.

p. 8414, line 17 and following: Would the size-resolved AMS chemistry data not be more helpful here, rather than the bulk organic fraction, which surely is more sensitive to larger particles?

Response:

We analyzed the size-resolved AMS data. The response is given above.

p. 8414, line 20: “considering that the chemical species contributing to particle growth was similar to: : :”: This is an assumption and should be stated as such.

Response:

It was removed from the text.

p. 8414, line 18: please define “later stage”

Response:

“later stage” is changed to be “a relatively later time of the NPF event”

****

Section 4.3:

p. 8415, line 12: “: : :..step-wisely enhanced due to the accumulation processing” It is not completely clear to me what is meant by that.

Response:

“During three consecutive NPF days, the CCN number concentration step-wisely enhanced due to the accumulation processing." was removed from the text.

p. 8415, line 17 "same time period before the end of the event": please define "end ofevent"

Response:

The starting and ending time of PNF events have been marked in the Fig.1 (a).

p. 8416, lines 22 – 24: Please substantiate the statement on BVOCs.

Response:

The VOCs measurements performed at Melpitz research station showed that VOCs are mainly biogenic volatile organic compounds. The following figure copied from a supplementary material of a recent publication (Mutzel et al., 2015) displayed the VOCs concentration during summertime at Melpitz station. It is very clear that the BVOCs are dominated in the atmosphere of Melpitz.

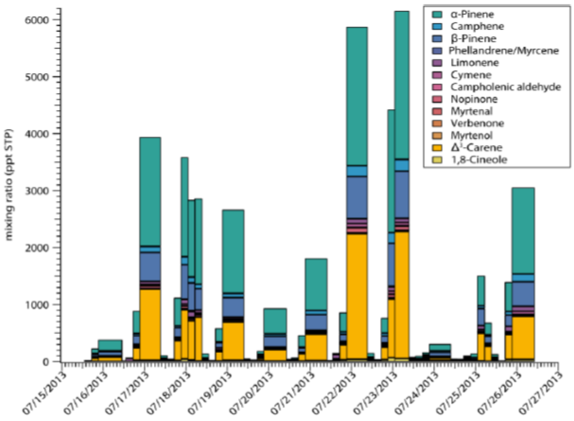

Figure S5. Time variation of the different VOC compounds sampled by TENAX cartridges. The width of each bar is covering the complete sampling period of each cartridge.

Modification in the MS:

At Melpitz, biological activities produced a lot of biogenic volatile organic compounds (BVOCs) (Mutzel et al., 2015) and lead to an organic-rich environment during summertime. The oxidation products of BVOCs may be responsible for the new particle growth.

p. 8417, line 14: "The observation showed that: : :." This does not follow from the observations presented in this study.

Response:

"The observation showed that sulfuric acid is a key species of atmospheric nucleation." was removed from the conclusions.

****

Comments on the Tables and Figures:

Table 1: What measurement points or what averages over which time frames are shown here?

Response:

In table 1, the equivalent water-soluble fraction 35, 50, and 75 nm particles is corresponding to the HTDMA measurement points at which the mean geometric diameter (Dm) of ultrafine particle mode reached 35, 50, and 75 nm.

Modifications in the MS:

One sentence was added into the MS "Here, the equivalent water-soluble fraction is corresponding to the HTDMA measurement points at which the mean geometric diameter (Dm) of ultrafine particle mode reached 35, 50, and 75 nm."

Figure 1: The figure is overloaded. It is vital to be able to read details out of Figure 1 to understand the text, but everything is very small. My suggestion would be to make three Figures (total): one with size distributions, critical diameter, and CCN concentrations,

a second one with chemical composition and hygroscopic growth factors, and a third with the auxiliary meteorological and gas-phase data.

a) The plot should not be this saturated (in both the upper and the lower concentration limit); a lot of detail is lost. A logarithmic concentration scale would help tremendously.

What are the white circles? The diameter axis should have minor ticks (numerous references to specific particle sizes in the text). The color bar label is in an odd place.

b) What is the unit of H_2SO_4? c) The RH axis should not extend to 120%.

Figure 2: It would be helpful if the beginning and end of the nucleation event were marked in the plot, in addition to t1 and t2.

Modifications in the MS:

Figures are replotted and added into the MS:

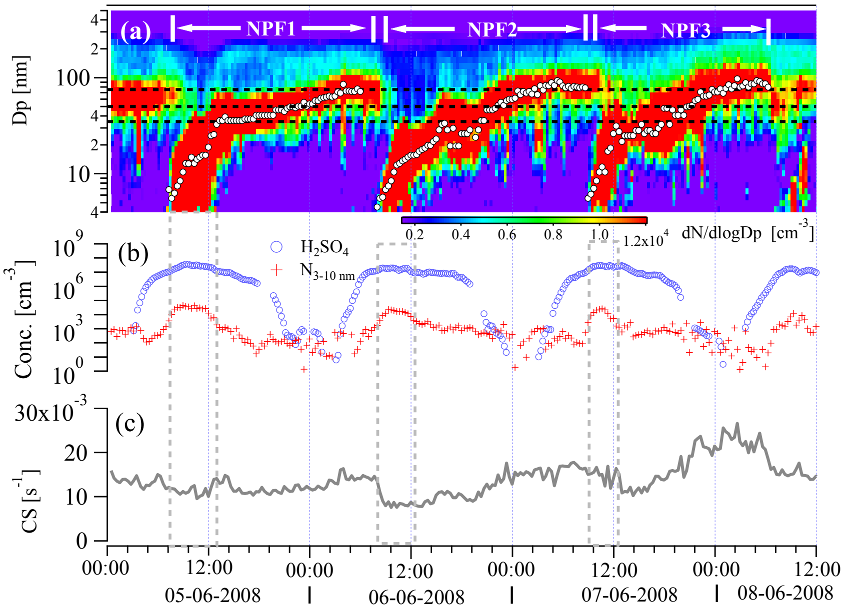

Fig. 1: Particle number size distribution, 3-10 nm particle number concentration, H_2SO_4 concentration, condensation sink (CS) during the NPF events. The starting and ending time of the events were marked in the upper place of panel (a) by NPF1, NPF2, and NPF3. The grey dashed lines indicated the time period of particle formation.

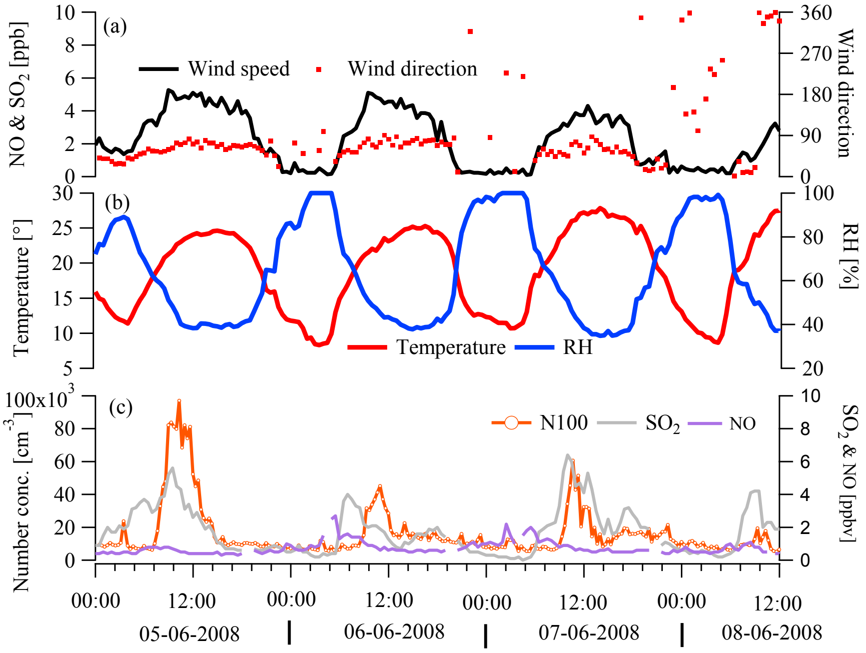

Fig. 2: The time series of wind speed and wind direction (a), ambient temperature and RH (b), and SO_2 & NO concentrations and number concentrations of particles in diameters of 3-100 nm (b).

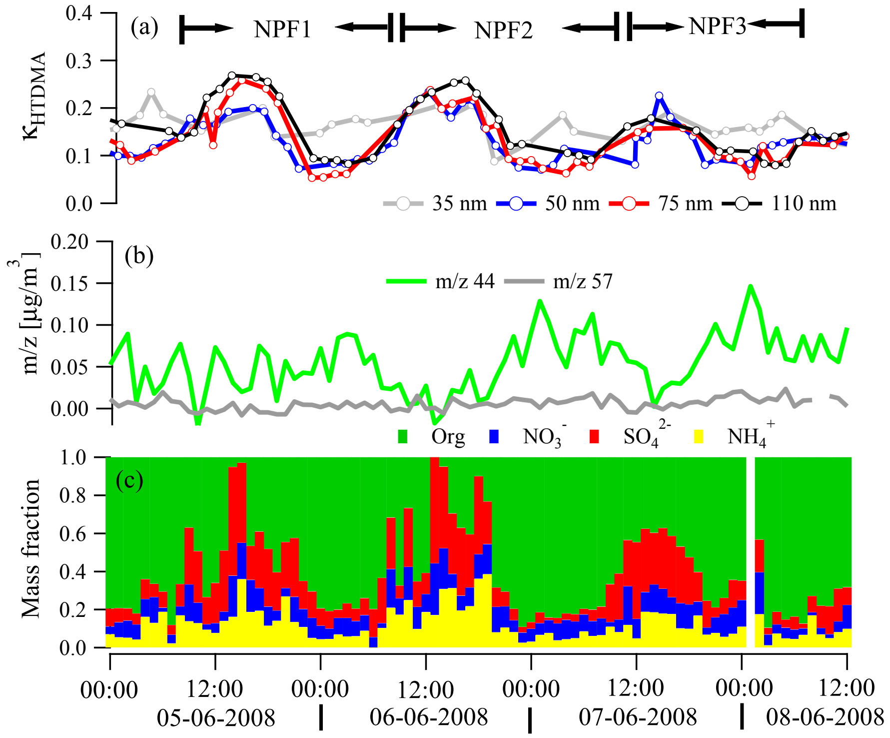

Fig.3: Size-resolved particle hygroscopicity (a), m/z 44 and 57 concentrations (b), and mass fraction of organic, sulfate, nitrate, and ammonium in 30-100 nm in mobility diameter (c).

Reference

Altstädter, B., Platis, A., Wehner, B., Scholtz, A., Wildmann, N., Hermann, M., Käthner, R., Baars, H., Bange, J., and Lampert, A.: ALADINA – an unmanned research aircraft for observing vertical and horizontal distributions of ultrafine particles within the atmospheric boundary layer, Atmos. Meas. Tech., 8, 1627-1639, 10.5194/amt-8-1627-2015, 2015.

Birmili, W., and Wiedensohler, A.: New particle formation in the continental boundary layer: Meteorological and gas phase parameter influence, Geophysical Research Letters, 27, 3325-3328, 10.1029/1999GL011221, 2000.

Boy, M., Rannik, Ü., Lehtinen, K. E. J., Tarvainen, V., Hakola, H., and Kulmala, M.: Nucleation events in the continental boundary layer: Long-term statistical analyses of aerosol relevant characteristics, Journal of Geophysical Research: Atmospheres, 108, n/a-n/a, 10.1029/2003JD003838, 2003.

Boy, M., Hellmuth, O., Korhonen, H., Nilsson, E. D., ReVelle, D., Turnipseed, A., Arnold, F., and Kulmala, M.: MALTE – model to predict new aerosol formation in the lower troposphere, Atmos. Chem. Phys., 6, 4499-4517, 10.5194/acp-6-4499-2006, 2006.

Canagaratna, M. R., Jayne, J. T., Jimenez, J. L., Allan, J. D., Alfarra, M. R., Zhang, Q., Onasch, T. B., Drewnick, F., Coe, H., Middlebrook, A., Delia, A., Williams, L. R., Trimborn, A. M., Northway, M. J., DeCarlo, P. F., Kolb, C. E., Davidovits, P., and Worsnop, D. R.: Chemical and microphysical characterization of ambient aerosols with the aerodyne aerosol mass spectrometer, Mass Spectrometry Reviews, 26, 185-222, 10.1002/mas.20115, 2007.

Cerully, K. M., Raatikainen, T., Lance, S., Tkacik, D., Tiitta, P., Petäjä, T., Ehn, M., Kulmala, M., Worsnop, D. R., Laaksonen, A., Smith, J. N., and Nenes, A.: Aerosol hygroscopicity and CCN activation kinetics in a boreal forest environment during the 2007 EUCAARI campaign, Atmos. Chem. Phys., 11, 12369-12386, 10.5194/acp-11-12369-2011, 2011.

Dal Maso, M., Kulmala, M., Riipinen, I., Wagner, R., Hussein, T., Aalto, P. P., and Lehtinen, K. E.: Formation and growth of fresh atmospheric aerosols: eight years of aerosol size distribution data from SMEAR II, Hyytiala, Finland, Boreal Environment Research, 10, 323, 2005.

Good, N., Topping, D. O., Allan, J. D., Flynn, M., Fuentes, E., Irwin, M., Williams, P. I., Coe, H., and McFiggans, G.: Consistency between parameterisations of aerosol hygroscopicity and CCN activity during the RHaMBLe discovery cruise, Atmos. Chem. Phys., 10, 3189-3203, 10.5194/acp-10-3189-2010, 2010.

Gysel, M., Crosier, J., Topping, D. O., Whitehead, J. D., Bower, K. N., Cubison, M. J., Williams, P. I., Flynn, M. J., McFiggans, G. B., and Coe, H.: Closure study between chemical composition and hygroscopic growth of aerosol particles during TORCH2, Atmos. Chem. Phys., 7, 6131-6144, 10.5194/acp-7-6131-2007, 2007.

Gysel, M., McFiggans, G. B., and Coe, H.: Inversion of tandem differential mobility analyser (TDMA) measurements, Journal of Aerosol Science, 40, 134-151, 10.1016/j.jaerosci.2008.07.013, 2009.

Hamed, A., Birmili, W., Joutsensaari, J., Mikkonen, S., Asmi, A., Wehner, B., Spindler, G., Jaatinen, A., Wiedensohler, A., Korhonen, H., Lehtinen, K. E. J., and Laaksonen, A.: Changes in the production rate of secondary aerosol particles in Central Europe in view of decreasing SO2 emissions between 1996 and 2006, Atmos. Chem. Phys., 10, 1071-1091, 10.5194/acp-10-1071-2010, 2010.

Heintzenberg, J.: Properties of the Log-Normal Particle Size Distribution, Aerosol Science and Technology, 21, 46-48, 10.1080/02786829408959695, 1994.

Hussein, T., Aalto, P. P., and Lehtinen, K. E. J.: Formation and growth of fresh atmospheric aerosols: eight years of aerosol size distribution data from SMEAR II, Hyytiälä, Finland, 2000.

Irwin, M., Good, N., Crosier, J., Choularton, T. W., and McFiggans, G.: Reconciliation of measurements of hygroscopic growth and critical supersaturation of aerosol particles in central Germany, Atmos. Chem. Phys., 10, 11737-11752, 10.5194/acp-10-11737-2010, 2010.

Janhäll, S., M. Jonsson, Å., Molnár, P., A. Svensson, E., and Hallquist, M.: Size resolved traffic emission factors of submicrometer particles, Atmospheric Environment, 38, 4331-4340, http://dx.doi.org/10.1016/j.atmosenv.2004.04.018, 2004.

Mutzel, A., Poulain, L., Berndt, T., Iinuma, Y., Rodigast, M., Böge, O., Richters, S., Spindler, G., Sipilä, M., Jokinen, T., Kulmala, M., and Herrmann, H.: Highly Oxidized Multifunctional Organic Compounds Observed in Tropospheric Particles: A Field and Laboratory Study, Environmental Science & Technology, 49, 7754-7761, 10.1021/acs.est.5b00885, 2015.

Petters, M. D., and Kreidenweis, S. M.: A single parameter representation of hygroscopic growth and cloud condensation nucleus activity, Atmos. Chem. Phys., 7, 1961-1971, 10.5194/acp-7-1961-2007, 2007.

Petters, M. D., Wex, H., Carrico, C. M., Hallbauer, E., Massling, A., McMeeking, G. R., Poulain, L., Wu, Z., Kreidenweis, S. M., and Stratmann, F.: Towards closing the gap between hygroscopic growth and activation for secondary organic aerosol – Part 2: Theoretical approaches, Atmos. Chem. Phys., 9, 3999-4009, 10.5194/acp-9-3999-2009, 2009.

Poulain, L., Birmili, W., Canonaco, F., Crippa, M., Wu, Z. J., Nordmann, S., Spindler, G., Prévôt, A. S. H., Wiedensohler, A., and Herrmann, H.: Chemical mass balance of 300 °C non-volatile particles at the tropospheric research site Melpitz, Germany, Atmos. Chem. Phys., 14, 10145-10162, 10.5194/acp-14-10145-2014, 2014.

Wex, H., Petters, M. D., Carrico, C. M., Hallbauer, E., Massling, A., McMeeking, G. R., Poulain, L., Wu, Z., Kreidenweis, S. M., and Stratmann, F.: Towards closing the gap between hygroscopic growth and activation for secondary organic aerosol: Part 1 – Evidence from measurements, Atmos. Chem. Phys., 9, 3987-3997, 10.5194/acp-9-3987-2009, 2009.

Wu, Z. J., Poulain, L., Henning, S., Dieckmann, K., Birmili, W., Merkel, M., van Pinxteren, D., Spindler, G., Mueller, K., Stratmann, F., Herrmann, H., and Wiedensohler, A.: Relating particle hygroscopicity and CCN activity to chemical composition during the HCCT-2010 field campaign, Atmospheric Chemistry and Physics, 13, 7983-7996, 10.5194/acp-13-7983-2013, 2013.

Zhang, Q., Stanier, C. O., Canagaratna, M. R., Jayne, J. T., Worsnop, D. R., Pandis, S. N., and Jimenez, J. L.: Insights into the Chemistry of New Particle Formation and Growth Events in Pittsburgh Based on Aerosol Mass Spectrometry, Environmental Science & Technology, 38, 4797-4809, 10.1021/es035417u, 2004.

Zhu, Y., Hinds, W. C., Kim, S., and Sioutas, C.: Concentration and Size Distribution of Ultrafine Particles Near a Major Highway, Journal of the Air & Waste Management Association, 52, 1032-1042, 10.1080/10473289.2002.10470842, 2002.

Some insights into the condensing vapors driving new particle growth to CCN sizes on the basis of hygroscopicity measurements

Z. J. Wu[1,2], L. Poulain[2], W. Birmili[2], J. Größ[2], N. Niedermeier[2], Z. B. Wang[3], H. Herrmann[2], A. Wiedensohler[2]

[1] College of Environmental Sciences and Engineering, Peking University, 100871, Beijing, China

[2] Leibniz Institute for Tropospheric Research, 04318, Leipzig, Germany

[3] Multiphase Chemistry Department, Max Planck Institute for Chemistry, Mainz 55128, Germany

Correspondence to: Zhijun Wu (zhijunwu@pku.edu.cn)

Abstract

New particle formation (NPF) and growth is an important source of cloud condensation nuclei (CCN). In this study, we investigated the chemical species driving new particle growth to the CCN sizes on the basis of particle hygroscopicity measurements carried out at the research station Melpitz, Germany. Three consecutive NPF events occurred during summertime were chosen as examples to perform the study. Hygroscopicity measurements showed that the $(NH_4)_2SO_4$-equivalent water-soluble fraction respectively accounts for 20% and 16% of 50 and 75 nm particles during the NPF events. Numerical analysis showed the ratios of H_2SO_4 condensational growth to the observed particle growth were 20% and 13% for 50 and 75 nm newly formed particles, respectively. Aerosol mass spectrometer measurements showed that the sulfate and ammonium were dominated in the mass fraction of 30-100 nm particles at an earlier time of the NPF event. At a later time, the secondary organic species played a key role in the particle growth. Both hygroscopicity and AMS measurements and numerical analysis confirmed that organic compounds were major contributors driving particle growth to CCN sizes. The critical diameters at different supersaturations estimated using AMS data and κ-Köhler theory increased significantly during the later course of NPF events. This indicated that the enhanced organic mass fraction caused a reduction in CCN efficiency of newly formed particles. Our results implied that the CCN production associated with atmospheric nucleation may be overestimated if assuming that newly formed particles can serve as CCN in case they grow to a fixed particle size, which was used in some previous studies, especially for organic-rich environments. In our study, the enhancement in CCN number concentration associated with

individual NPF events have been 63%, 66%, and 69% for supersaturation 0.1%, 0.4%, and 0.6%, respectively.

1 Introduction

The formation of new particles from gaseous precursors and their subsequent growth represent a key stage in the lifecycle of atmospheric aerosol particles. This new particle formation (NPF) process represents an important source of atmospheric particles and possibly also for the number concentration of potential cloud condensation nuclei (CCN) (Spracklen et al., 2008;Wiedensohler et al., 2009;Wang and Penner, 2009;Laaksonen et al., 2005;Yue et al., 2011;Kazil et al., 2010;Sotiropoulou et al., 2006;Laakso et al., 2013) . NPF has thus the potential to influence climatologically important processes such as precipitation patterns and Earth's energy balance (Paasonen et al., 2013). The contribution of atmospheric nucleation to the global CCN budget spans a relatively large uncertainty range, which, together with our general poor understanding of aerosol-cloud interactions, results in major uncertainties in the radiative forcing by atmospheric aerosols (Kerminen et al., 2012). Recent model studies (Spracklen et al., 2008;Merikanto et al., 2009;Westervelt et al., 2014) have attempted to elaborate on the connection between NPF and CCN production, a process that is sensitive to a number of environmental factors.

Freshly formed particles are about 1 nanometers in diameter (Kulmala et al., 2012), and they must grow tens of nanometers in order to serve as a CCN (Dusek et al., 2006;Kerminen et al., 2012). Apparently, the nucleation rate, the particle growth and the rate by which growing particles are removed by coagulation or deposition greatly influence the CCN production associated with atmospheric nucleation (Kuang et al., 2009;Kerminen et al., 2004). From the point of view of chemical species, both sulfuric acid and organics contribute to the subsequent particle growth after nucleation (Smith et al., 2004;Pierce et al., 2011;Ehn et al., 2007;Kulmala et al., 2004;Brus et al., 2011;Kulmala et al., 2006;Sipilä et al., 2010;Zhang et al., 2004b;Kiendler-Scharr et al., 2009;Wang et al., 2010;Ristovski et al., 2010). The contribution of sulfate and organics in the particle growth seems to be strongly depending on the location (e.g. Yue et al., 2010;Boy et al., 2005). For example, sulfuric acid fully explains the particle growth observed in the polluted urban areas, Atlanta, USA (Stolzenburg et al., 2005), while it represents only 10% in Boreal forest area (Boy et al., 2005).

Due to the differences in hygroscopicity of sulfuric acid and/or its ammonium salts and secondary organic compounds (Virkkula et al., 1999;Varutbangkul et al., 2006;Tang and Munkelwitz, 1994), hygroscopicity measurements during a NPF event can provide insight into the changes in condensing vapor properties and chemical composition of newly formed particles (Hämeri et al., 2001;Ehn et al., 2007;Ristovski et al., 2010). In this study, we investigated the chemical species driving new particle growth into CCN sizes by using experimental data on particle hygroscopicity and chemical composition measured at Melpitz, Germany. In addition, the production of potential CCN associated with the NPF event was evaluated.

2 Measurements

Atmospheric measurements were performed at the research station Melpitz, Germany (51.54ºN, 12.93ºE, 86 m above sea level). The atmospheric aerosol observed at Melpitz can be regarded as representative for Central European background conditions (Birmili et al., 2009). An account of the NPF process at Melpitz and its relationship with precursor gases and meteorology can be found in Größ et al. (2015).

The data of this study were collected during the European Integrated Project on Aerosol Cloud Climate Air Quality Interactions (EUCAARI, (Kulmala et al., 2009)) intensive field campaign from May 23rd to June 8th in 2008. Table 1 summarizes the instruments and measured parameters used in this study. All instruments were set up in the same container laboratory and utilized the same air inlet. The inlet line consisted of a PM_{10} Anderson impactor located approximately 6 m above ground level and directly followed by an automatic aerosol diffusion dryer (Tuch et al., 2009) that maintained the relative humidity in the sampling line below 30%. Particle hygroscopicity, particle number size distribution, and chemical composition of non-refractory PM_1 were determined using a hygroscopicity tandem differential mobility particle analyzer (H-TDMA), a Twin Differential Mobility Particle Sizer (TDMPS), and a High Resolution Time-of-flight Aerosol Mass Spectrometer (HR-Tof-AMS), respectively.

2.1 Particle hygroscopicity measurements

The H-TDMA used in this study has been described in previous publications in detail (Wu et al., 2011;Massling et al., 2003), and complies to the instrumental standards prescribed in Massling et al. (2011). The H-TDMA consists of three main parts: (1) A Differential Mobility Analyzer (DMA1) that selects quasi-monodisperse particles at a relative humidity below 10%, and a

Condensation Particle Counter (CPC1) that measures the particle number concentration leaving DMA1 at the selected particle size; (2) An aerosol humidifier conditioning the particles selected by DMA1 to a defined relative humidity (RH); (3) The second DMA (DMA2) coupled with another condensation particle counter (CPC2) to measure the number size distributions of the humidified aerosol. DMA2 and the aerosol humidification are placed in a temperature-controlled box. Hygroscopicity scans with 100 nm ammonium sulfate particles were performed frequently to analyze the stability of the relative humidity of 90% in the second DMA. Hygroscopicity scans with a deviation of more than 3% in relative humidity from the set-point of 90% were not considered for further analysis.

The hygroscopic growth factor (HGF) is defined as the ratio of the particle mobility diameter, Dp(RH), at a given RH to the dry diameter, Dp_{dry}:

$$\mathrm{HGF(RH)} = \frac{\mathrm{D_p(RH)}}{\mathrm{D_{p_{dry}}}} \qquad [1]$$

The TDMAinv method developed by Gysel et al. (2009) was used to invert the H-TDMA data. Dry scans (RH<10%) were used to calibrate a possible offset between DMA1 and DMA2 and define the width of the H-TDMA's transfer function (Gysel et al., 2009). In this study, the particles with dry sizes of 35, 50, 75, 110, 165, and 265 nm were measured by H-TDMA at RH=90% with the time resolution of 1h. The HGFs of 35, 50, and 75 nm particles will be taken for further analysis.

The hygroscopicity parameter, κ, can be calculated from the HGF measured by H-TDMA (Petters and Kreidenweis, 2007):

$$\kappa_{\mathrm{HTDMA}} = (\mathrm{HGF}^3 - 1)\left(\frac{\exp\left(\frac{\mathrm{A}}{\mathrm{D_{p_{dry}}}\cdot\mathrm{HGF}}\right)}{\mathrm{RH}} - 1\right) \qquad [2]$$

$$\mathrm{A} = \frac{4\sigma_{s/a}\mathrm{M_w}}{\mathrm{RT}\rho_w} \qquad [3]$$

Where D_{Pdry} and HGF are the initial dry particle diameter and the hygroscopic growth factor at 90% RH measured by H-TDMA, respectively. $\sigma_{s/a}$ is the droplet surface tension (assumed to be that of pure water, $\sigma_{s/a}$ =0.0728 N m^{-2}), M_w the molecular weight of water, ρ_w the density of liquid water, R the universal gas constant, and T the absolute temperature.

2.2 Particle chemical composition

The Aerodyne HR-ToF-AMS (here simply referred to as AMS) (DeCarlo et al., 2006) was operated with a time resolution of 5 min. Due to the 600 ˚C surface temperature of the vaporizer, the AMS only analyzes the non-refractory chemical composition of the particles. Soot, crustal material, and sea-salt cannot be detected. The aerodynamic lenses have 100% transmission efficiency down to 70 nm in a vacuum aerodynamic diameter (Canagaratna et al., 2007). Therefore, based on the transmission efficiency of the aerodynamic lenses and the detected compounds, the AMS can provide the size-resolved chemical composition of sub-micrometer non-refractory aerosol particle fraction (NR-PM1) (Canagaratna et al., 2007). The vacuum aerodynamic diameter for AMS measurements was converted to mobility diameter by division of AMS vacuum aerodynamic diameter by the estimated particle density (1400 kg/m^3). Hereafter, the mobility diameter is used in AMS data below. The particle density was calculated on the basis of measured chemical composition. The detail description about the calculation was given in Poulain et al. (2014).

2.3 Particle number size distribution

A TDMPS was deployed to measure particle number size distributions from 3-800 nm mobility diameter with a time resolution of 10 min (Birmili et al., 1999). The system consists of two Differential Mobility Analyzers (DMA, Hauke-type) and two Condensation Particle Counters (CPC, TSI model 3010 and TSI model 3025). The sheath air is circulated in closed loops for both DMAs. Evaluation of particle number size distributions includes a multiple charge inversion, the CPC efficiency and diffusional losses in the DMA and all internal and external sampling lines according to the recommendations in Wiedensohler et al. (2012).

3 Methodology

3.1 Derivation of the soluble particle fraction

Based on the Zdanovskii–Stokes–Robinson (ZSR) method (Stokes and Robinson, 1966;Zdanovskii, 1948), the HGF of a mixture can be estimated from the sum of HGF_i of a pure component (i) time their respective volume fractions, ε_i (Malm and Kreidenweis, 1997):

$$\mathrm{HGF}_{\mathrm{mixed}} = \left(\sum_i \varepsilon_i \mathrm{HGF}_i^3\right)^{1/3} \qquad [4]$$

Here, the chemical compounds contributing to the particle growth are separated into two fractions, e.g., soluble and insoluble fractions (also refer to Ehn et al., 2007;Swietlicki et al., 1999). The soluble fraction is assumed as ammonium sulfate and the insoluble fraction as organic compounds. Then, ε of soluble fraction can be calculated by:

$$\varepsilon_{\mathrm{soluble}} = \frac{\mathrm{HGF}_{\mathrm{measured}}^3 - 1}{\mathrm{HGF}_{(\mathrm{NH_4})_2\mathrm{SO_4}}^3 - 1} \qquad [5]$$

where $\mathrm{HGF}_{\mathrm{measured}}$ is the HGF of particle measured by H-TDMA, and $\mathrm{HGF}_{(\mathrm{NH_4})_2\mathrm{SO_4}}$ is the HGF of pure $(NH_4)_2SO_4$ particle with the same size. When calculating $\mathrm{HGF}_{(\mathrm{NH_4})_2\mathrm{SO_4}}$ in different diameters, the parameterizations for $(NH_4)_2SO_4$ water activity developed by Potukuchi and Wexler (1995) and the density reported by Tang and Munkelwitz (1994) are used. The Kelvin term was considered in the calculation.

The assumption of an insoluble organic fraction may lead to overestimate of the soluble fraction because atmospherically relevant secondary organics typically have a growth factor larger than 1 (e.g., Varutbangkul et al., 2006). This implies that in the presence of several classes of hygroscopic substances. ε derived from Eq. [5] is only an “equivalent” soluble fraction (i.e. assuming ammonium sulfate as the only soluble substance). $\varepsilon_{\mathrm{soluble}}$ is therefore an upper estimate for the true soluble volume fraction. The advantage of using the equivalent water-soluble fraction term is to be able to analyze the particle hygroscopicity independently of differences in size. The uncertainty of the estimated soluble volume fraction is around 5%, which was derived from the measurement uncertainty of HGF (2.5%) according to the error propagation function.

3.2 Calculation of CCN number concentration

The CCN number concentration can be estimated by integrating the particle number size distribution from the critical diameter to the maximum diameter detected by TDMPS (800 nm, above which the particle number concentration is generally negligible), assuming particles are internal mixture. The critical diameter (D_{pcrit}) is calculated from κ:

$$D_{\mathrm{Pcrit}} = \left(\frac{4A^3}{27\,\kappa_{\mathrm{chem}} \ln^2 S_C}\right)^{1/3} \qquad [6]$$

Here, D_{Pcrit} is the critical diameter at which 50% of the particles were activated at the supersaturation, S_c (0.1%, 0.4%, and 0.6% were chosen in this study). κ_{chem} is calculated from size-resolved AMS data according to the ZSR method and κ-Köhler theory (Petters and Kreidenweis, 2007):

$$\kappa_{\mathrm{chem}} = \sum_i \varepsilon_i \kappa_i \qquad [7]$$

Here, κ_i and ε_i are the hygroscopicity parameter and volume fraction for the individual (dry) component in the mixture with *i*, the number of components in the mixture. The volume fraction of each chemical species in the mixture was derived from the size-resolved AMS data as described below.

Particle mass size distributions of organics, sulfate (SO_4^{2-}), nitrate (NO_3^-), and ammonium (NH_4^+) ions were detected by AMS. We use a simplified ion pairing scheme as presented in Gysel et al. (2007) to convert the ion mass concentrations to the mass concentrations of their corresponding inorganic salts as listed in Table 2. The critical diameters, corresponding to supersaturation (SS) 0.2-0.6%, roughly spanned from 50 to 120 nm in mobility diameter. Therefore, by integrating the particle mass size distribution from 50 nm to 120 nm, the mass concentrations of organics, SO_4^{2-}, NO_3^-, and NH_4^+ ions was calculated to estimate κ_{chem}. In the same way, the chemical composition of 150-200 nm particles is used to calculate κ_{chem} for the critical diameter of around 170 nm, which corresponds to a supersaturation of 0.1%.

The H-TDMA-derived κ was not used in calculating the critical diameter. This reason was given as follow: The inconsistencies between H-TDMA-derived kappa and Cloud Condensation Nuclei Counter (CCNc)-derived κ have been reported in several previous studies (Good et al., 2010;Cerully et al., 2011;Irwin et al., 2010;Petters et al., 2009;Wex et al., 2009). Possible explanations are non-ideality effects in the solution droplet, surface tension reduction due to surface active substances, and the presence of slightly soluble substances which dissolve at RHs larger than the one considered in the H-TDMA (Wex et al., 2009). Due to these effects, κ is not necessarily constant and may vary with humidity. Extrapolating from H-TDMA data to properties at the point of activation should be done with great care (Wu et al., 2013). In addition, our previous study (Wu et al., 2013) showed that critical diameters at different supersaturations can be well-predicted using AMS data and ZSR method. Therefore, the AMS data was decided to use to estimate the critical diameters instead of H-TDMA-derived κ.

3.3 Estimation of H_2SO_4 concentration

H_2SO_4 concentrations were estimated using a modified version of the chemical mass balance model introduced by Weber et al. (1997), driven by solar radiation as a source of OH:

$$[\mathrm{H_2SO_4}] = \mathrm{B}\frac{[\cdot\mathrm{OH}][\mathrm{SO_2}]}{\mathrm{CS}} \quad [\mathrm{cm^{-3}}] \qquad [8]$$

Here, [·OH] is the hydroxyl radical concentration estimated from Eq. [9] in cm^{-3}. $[SO_2]$ is the measured sulfur dioxide concentration in cm^{-3}. *B* is a constant related to the reaction rate of the two species. CS is the condensation sink (Pirjola et al., 1999) in s^{-1} calculated from the particle number size distribution adjusted to ambient relative humidity. For this adjustment, an empirical growth law based on one year of hygroscopicity measurements at Melpitz was used (Refer to Laakso et al., 2004). The term $B[\cdot OH][SO_2]$ represents the production term of H_2SO_4, and CS is referred to represent the loss rate of H_2SO_4 on the pre-existing particles. B was derived by correlation analysis of measured and estimated $[H_2SO_4]$ for 9 days during EUCAARI-2008 during which the data capture was satisfactory. Linear regression analysis yielded a value of $27.49 \cdot 10^{-13}$ cm^3 s^{-1} for B.

$$[\cdot\,\mathrm{OH}] = \mathrm{A'}\cdot\mathrm{Rad} \quad [\mathrm{cm^{-3}}] \qquad [9]$$

where Rad is the global solar radiation flux in W m^{-2}. A′ was derived by linear regression of these parameters for the EUCAARI-2008 data set, yielding a value of 6166 m^2 W^{-1} for A′. The calculation of H_2SO_4 concentration was done within the works of Größ et al. (2015), with details provided therein. The accuracy of simulated H_2SO_4 concentration is estimated as follow: Percentage error = abs ($[H_2SO_4]_{measured}$ - $[H_2SO_4]_{simulated}$) * 100 / $[H_2SO_4]_{simulated}$. Here, $[H_2SO_4]_{measured}$ is the sulfuric acid concentration measured during 9-day measurements for EUCAARI-2008. The percentage error is around 40%.

3.4 Calculation of particle formation and growth rate

Assuming a constant particle source during a time period of t, the particle formation rate (J_{nuc}) can be expressed as (Dal Maso et al., 2005):

$$\mathrm{J_{nuc}} = \frac{\mathrm{dN_{nuc}}}{\mathrm{dt}} + \mathrm{F_{coag}} + \mathrm{F_{growth}} \qquad [10]$$

In this study, N_{nuc} is the number concentration of nucleation mode particles ranging from 3 nm to 25 nm. F_{growth} is the flux of particles out of the specified size range (3-25 nm). The newly formed particles rarely grew beyond 25 nm before formation ended, and F_{growth} can be neglected. F_{coag} represents a loss of formed particles due to coagulation to the preexisting particle population. It can be calculated from the following equation:

$$\mathrm{F_{coag} = CoagS_{nuc}N_{nuc}} \qquad [11]$$

where $CoagS_{nuc}$ is the coagulation sink of particles in the nucleation mode. The detailed calculation of coagulation sink is given in Deal Maso et al. (2005).

The observed particle growth rate (GR_{obs}) can be expressed as:

$$\mathrm{GR_{obs}} = \frac{\Delta \mathrm{D_m}}{\Delta \mathrm{t}} \qquad [12]$$

where Dm is a mean geometric diameter of log-normal ultrafine particle mode, which has been fitted to the number size distribution (Heintzenberg, 1994). GR_{obs} means evolution of the mean diameter within a time period Δt.

3.5 Particle growth contributed by H_2SO_4 condensation

Theoretically, the vapor concentration required for growth rate of 1 nm h^{-1} in certain particle size ranges can be calculated according to (Nieminen et al., 2010):

$$C_{GR=1nm/h} = \frac{2\rho_v d_v}{\gamma m_v \Delta t} \cdot \sqrt{\frac{\pi m_v}{8kT}} \cdot \left[\frac{2x_1+1}{x_1(x_1+1)} - \frac{2x_0+1}{x_0(x_0+1)} + 2ln\left(\frac{x_1(x_0+1)}{x_0(x_1+1)}\right)\right] \qquad [13]$$

here x_0 and x_1 are the ratios of the vapour molecule diameter (d_v) to the initial and final particle diameter, respectively. The mass (m_v) and density (ρ_v) of sulfuric acid applied in this study are 135 amu and 1650 kg/m^3, respectively, corresponding to hydrated sulfuric acid molecules (Kurtén et al., 2007). It should be mentioned that equation [13] was developed specially for particles with diameter of 3-7 nm. For larger particles (>10 nm), this method gives similar results to that calculated using the Fuchs-Sutugin approach (Nieminen et al., 2010). The calculated $C_{GR=1\mathrm{nm/h},H_2SO_4}$ may be an underestimate because it is assumed that every sulfuric acid molecule colliding with the particle is attached to it which is not necessarily the case.

Then the growth rate contributed by sulfuric acid during the time period used for the determination of GR is calculated directly as:

$$\mathrm{GR}_{\mathrm{H_2SO_4}} = [\mathrm{H_2SO_4}]_{\mathrm{est}} / C_{\mathrm{GR=1nm/h,\,H_2SO_4}} \qquad [14]$$

where $[\mathrm{H_2SO_4}]_{\mathrm{est}}$is the median value from the estimated sulfuric acid concentration during the timeframe for the determination of GR.

The observed growth rate can be presented as the sum of the growth rates due to H_2SO_4 (GR_{H2SO4}) and organic vapors (GR_{org}) condensation (Paasonen et al., 2010):

$$\mathrm{GR}_{\mathrm{obs}} = \mathrm{GR}_{\mathrm{H_2SO_4}} + \mathrm{GR}_{\mathrm{Org}} \qquad [15]$$

By combining equations [13-15], the overall particle volume change can be separated into two fraction contributing by H_2SO_4 and organic vapors condensation.

4 Results

4.1 Particle formation and growth

The previous study on the basis of long-term observations showed that the NPF events take place frequently at Melpitz, especially on April, May, and June (Hamed et al., 2010). During our field campaign (from May 23rd to June 8th in 2008), the NPF events were also observed frequently. In present study, three NPF events, which consecutively took place from June 5 to June 7, 2008, as displayed in Fig. 1 (a), are selected for further analysis. These events are the best cases which showed clear particle bursts and subsequent growth process during the entire field campaign. The starting and ending time for each event were marked in the Fig.1 (a) as NPF1, NPF2, and NPF3. The bursts in number concentration of 3-10 nm particles were observed associated with increasing ambient temperature, decreasing relative humidity (shown in Fig. 2 (b)), and increasing in estimated H_2SO_4 concentration (shown in Fig. 1(b)). The CS is between 0.01 and 0.02 s^{-1} during the NPF events. As marked in Fig.1 (a), the particle number size distribution shows the new particle formed around 10:00 a.m. and then grew versus time for more than 20 h. This means that the NPF is a regional event (refere to Hussein et al., 2000) and could take place over a distance of a hundred kilometers. The Fig.2 (a) displays the wind speed and wind direction during the NPF events. The wind showed a typical diurnal cycle. The wind speed was 4-5 m/s and kept a constant direction (south) during the daytime. It was static wind during nighttime. The particle formation rates ($J_{3\text{-}25nm}$) were 13.5, 6.1, 9.3 $cm^{-3}s^{-1}$ on June 5, 6, and 7, respectively. The highest formation rate was observed on June 5 corresponding to the highest H_2SO_4 concentration.

As indicated by the white circle in the Fig.1 (a), the mean geometric diameter (D_m) of log-normal ultrafine particle mode increased to around 100 nm within 24 hours. Over the time period from the beginning to the end of the NPF events as marked in Fig.1 (a), the average GR_{obs}s were respectively 2.8, 3.6, and 4.4 nm h^{-1} for NPF events on June 5th, 6th, and 7th, 2008. One can note that the newly formed particles continued growing during the nighttime when sulfuric acid concentration was close to zero. This indicated that other species, most likely, organic compounds contributed to the particle growth during this time period.

There were no local emission sources in the surrounding areas of the Melpitz research station. The possible primary emissions contributing to the atmospheric particles at Melpitz could be from the cities away tens of kilometers from the station via transportation. Typically, the primary particles are accompanied by trace gases, such as NO and SO_2 spikes. However, such phenomena were not observed in our measurements at Melpitz. As shown in Fig.2 (c), in the early morning on 6 and 7 June, the slight enhancement of NO (a tracer for traffic related ultrafine particles (Janhäll et al., 2004)) concentration may be caused by the outflow of cities nearby Melpitz. The particle number concentration did not increased simultaneously. The ultrafine particles exhausted from car tailpipes in the cities may grow by condensation and coagulation and shift towards larger diameters and diluted by fresh air significantly with increasing distance from the roads (Zhu et al., 2002). As a result, the enhancement in ultrafine particle number concentration was not observed at the rural site of Melpitz. Therefore, the instant impacts of primary emissions on atmospheric particles were not observed during the time period focused in this study. SO_2 from primary emissions could contribute to the atmospheric nucleation after being oxidized to sulfuric acid by radicals. The new particle formation associating with enhanced SO_2 concentration was observed by many previous studies (e.g. Birmili and Wiedensohler, 2000). Overall, the new particle formation and subsequent growth is the major source of particles, and thereby, CCN at Melpitz station.

4.2 Hygroscopicity and chemical composition of newly formed particles

Fig.3 displayed the size-resolved particle hygroscopicity (a), m/z 44 and 57 mass concentrations (b), and mass fraction of organic, sulfate, nitrate, and ammonium in 30-100 nm (mobility diameter) particles (c). As shown in the Fig. 3(a), peak daily κs of 50, 75, and 110 nm particles occurred afternoon and minimum appeared in the midnight. The evolution of particle hygroscopicity was very similar to those of inorganic mass fraction (sulfate+nitrate+ ammonium) in 30-100 nm particles. During the daytime, H_2SO_4 concentration increased and may condense onto the particles. At the same time, the increasing ambient temperature (see Fig. 2 (b)) could drive the semi-volatile organic species in particle phase to partition to gas phase. Both processes could result in an increasing of inorganic fraction in particle phase, thereby enhancement in particle hygroscopicity. The decline in particle hygroscopicity took place after 15:30 (Local time) when sulfuric acid concentration decreased significantly. Simultaneously, ambient temperature decreased to 10˚C. Lower temperature facilitates the condensation of semi-volatile organic vapors onto the particles. As a result, the organic mass fraction increased significantly during the nighttime, as shown by AMS measurements (Fig.3 (c)), leading to an evident decline in particle hygroscopicity.

Table 3 summarizes the equivalent water-soluble fraction of newly formed particles when these particles grew to 35, 50, and 75 nm, respectively. Here, the equivalent water-soluble fraction is corresponding to the H-TDMA measurement points at which the mean geometric diameter (Dm) of ultrafine particle mode reached 35, 50, and 75 nm. On June 7, the equivalent water-soluble fraction of 35 nm newly formed particles was 34%. It decreased to 23% when particle grew to 50 nm, further, reduced to 17% when particles reached to 75 nm. On June 5 and 6, the hygroscopicity of newly formed particles decreased with increasing particle size, as well. It implies that a large fraction of species contributing to particle growth was organics, which are typically less water soluble. This can be confirmed by AMS measurements showing that organic fraction in particles increased at a relatively later time of the NPF event (see Fig. 3(c)). The contribution of H_2SO_4 condensation to particle growth was estimated using the method introduced in section 3.5 for different particle sizes. The ratios of H_2SO_4 condensational growth to the observed particle growth ($F_{GRH2SO4}=GR_{H2SO4}/GR_{obs}$) are given in the table 3. For example, on June 7, $F_{GRH2SO4}$ was 30% for 35 nm particles, meaning that H_2SO_4 condensation only contributed 30% of the observed particle growth. With increasing particle size, the contribution of H_2SO_4 condensation decreased, as shown in Table 3. This was consistent with the changes in the equivalent water-soluble fraction of newly formed particles. Both particle hygroscopicity measurements and numerical analysis showed that organics were major potential contributors to the particle growth.

As displayed in Fig.3 (c), the sulfate and ammonium were dominated in the inorganic mass fraction in 30-100 nm particles and obviously increased during the particle formation period (indicated by grey dashed line in Fig.1). While, the nitrate accounted for a minor fraction, which also observed by Zhang et al. in Pittsburgh (Zhang et al., 2004a). They found nitrate contributed the least to the new particle growth. After 3:00 p.m., the organic mass fraction increased and reached its maximum at midnight on each day, indicating that organics played a key role in the particle growth at a later time of the NPF event. The mass fraction of ion fragments m/z 44 and 57 in 30-100 nm particles are shown in the Fig. 3(b). The m/z 44 (CO_2^+ ion fragment) is a tracer for secondary organic aerosol， while m/z 57 ($C_4H_9^+$) is generally associated with primary organics from combustion sources (Zhang et al., 2004a). The m/z 57 mass concentration was close to zero during the events. Compared m/z 57, the m/z 44 mass concentration were considerable, indicating that the organics contributing to particle growth was mainly secondary organic species.

4.3 Enhancement in CCN number concentration during the NPF events

The critical diameters and CCN number concentrations at different supersaturations during the NPF events are displayed in the Fig. 4. The critical diameters at different supersaturations decreased during the first several hours of the NPF events and enhanced at a later time of the NPF event. This was consistent with the variations in particle hygroscopic growth at RH=90% above-mentioned (see Fig. 3(a)). As shown in the Fig. 4(b), the CCN number concentration clearly increased significantly during the NPF events. The minimum in CCN number concentration was observed during the period of particle formation and the maximum appeared at the end of the NPF events.

The NPF events occurred on June 5, 6, and 7 were typical regional cases. The enhancement in CCN number concentration caused by atmospheric nucleation was evaluated by comparing the average CCN number concentrations over two hours prior to the beginning of the event (the period t1 marked in Fig. 4) with the same time period before the end of the events (the period t2 marked in Fig. 4). The ratios of average CCN number concentration over t2 to t1 were respectively 1.9, 2.0, and 1.5 for 0.1%, 0.4%, and 0.6% SS. On average, the enhancement ratios in CCN number concentration associated with individual NPF events were 63%, 66%, and 69% for 0.1, 0.4, and 0.6% SS, respectively. The absolute increases in CCN number concentrations associated with each event were 162, 931, and 756 #/cm^3, on average.

Atmospheric boundary layer development and turbulent mixing will impact on NPF (Boy et al., 2006;Boy et al., 2003;Altstädter et al., 2015), and consequently on its CCN products. It is hard task to quantify the changes in CCN number due to boundary layer dynamics. In this study, the enhancement in CCN number concentration caused by atmospheric nucleation was evaluated by a ratio of CCN number during the same period on different days, and not an absolute value. Here we assume that the weather condition and boundary layer height were similar during two time periods (see meteorological parameters in Fig. 3). Therefore, the effect of boundary layer dynamics on the change in CCN number concentration could be ignored.

Several previous studies reported that the enhancement in CCN number concentration associated with atmospheric nucleation varied significantly in different environments. At the Finnish sub-Arctic Pallas station, a 210±110% increase in the number concentration of 80 nm particles was observed from the beginning of a nucleation event to the end of the event (Asmi et al., 2011). At a forested site (SMEAR II station in Hyytiälä) in Southern Finland, nucleation enhanced CCN number concentration by 70 to 110%, varying with the supersaturation level (Sihto et al., 2011). In a polluted urban area, Beijing, China, the average CCN enhancement factors were between about 1.5 and 2.5 (Yue et al., 2011;Wiedensohler et al., 2009). In Boulder, CO, Atlanta, GA, and Tecamac, Mexico, the pre-existing CCN number concentration increased on average by a factor of 3.8 as a result of new particle formation (Kuang et al., 2009). Overall, the enhancement in CCN number concentration associated with atmospheric nucleation varied significantly in different environments. Please note that the methods for defining the enhancement factors used in the existing literature were very different. Therefore, a general conclusion on how significant NPF and growth process contributes to CCN budget cannot be drawn, currently.

5 Discussion

The above field observations clearly showed that newly formed particles had the ability to grow into CCN sizes within several hours at Melpitz. The particle hygroscopicity measurements strongly suggested that organic compounds were the major contributors driving particle growth into CCN sizes. The previous studies performed in clean atmosphere also showed that the newly formed particles mainly consist of organics. For examples, sulfuric acid is able to account for roughly 30% of the growth rate of newly formed particles in the rural atmosphere of Hohenpeissenberg, Southern Germany (Birmili et al., 2003), and only around 10% in the boreal forest area of Finland (Boy et al., 2005). However, In the polluted atmosphere of Atlanta, USA, the available amount of sulfuric acid was sufficient to explain all of the observed particle growth (Stolzenburg et al., 2005). At Melpitz, biogenic volatile organic compounds (BVOCs) emitted from biological activities are dominated volatile organic compounds (Mutzel et al., 2015) and lead to an organic-rich environment during the summertime. The oxidation products of BVOCs may be responsible for the new particle growth.

We note that the condensation of organics lead to a rapid particle growth when sulfuric acid concentration was close to zero during the nighttime, as shown in Fig. 1. The organic condensing materials with low hygroscopicity reduced CCN efficiency of the new particles, as indicated by critical diameters given in Fig. 4. Such phenomenon was also reported by Dusek et al. (2010). They showed that enhanced organic mass fraction caused a reduction in CCN efficiency of small particles during the new particle formation. These results implied that the CCN production associated with atmospheric nucleation may be overestimated if assuming that new particles can serve as CCN in case they grow to a fixed particle size (Such as Asmi et al., 2011), especially for organic-rich environments. In our case, the mean critical diameter is around 50 nm at SS=0.6%. Assuming a constant critical diameter of 50 nm at SS=0.6%, the CCN number concentration was averagely 1.13 times of that with varied critical diameters during the NPF events. Under similar conditions, the CCN number concentration at SS=0.4% with a constant critical diameter of 70 nm was 1.15 times of that with varied critical diameters.

6 Conclusions

In this study, the particle number size distribution, particle hygroscopicity, and particle chemical composition during three regional NPF events were measured to investigate the new particle growth process and its effects on CCN activity. The particle formation rates ($J_{3\text{-}25nm}$) were 13.5, 6.1, 9.3 $cm^{-3}s^{-1}$, and the particle growth rates were 2.8, 3.6, and 4.4 nm/h for NPF events on June 5, 6 and 7, 2008, respectively.

The $(NH_4)_2SO_4$-equivalent water-soluble fraction accounted for 20% and 16% of 50 and 75 nm newly formed particles, respectively. The sulfate and ammonium were dominated in the mass fraction of 30-100 nm particles during the particle formation period. The nitrate contributed a minor fraction in new particle growth. At a later time of NPF event, the organics played a key role in the particle growth. The analysis on the fragment m/z 44 and 57 showed that the organics contributing to particle growth was mainly secondary organic species. The particle hygroscopicity and chemical composition measurements and numerical calculation confirmed that organic compounds were major contributors driving particles growth to CCN sizes.

The step-wised increase in CCN number concentration during three consecutive NPF events was observed. On average, the enhancement ratios in CCN number concentration associated with individual NPF events are 63%, 66%, 69% for 0.1, 0.4, and 0.6% SS, respectively. We found that the new particles hygroscopicity decreased significantly with condensational growth of organic compounds, which are generally less water soluble. Correspondingly, the critical diameters at a certain supersaturation increased, indicating that enhanced organic mass fraction caused a reduction in CCN efficiency of newly formed particles during the new particle formation. Our results implied that the CCN production associated with atmospheric nucleation may be overestimated if assuming that new particles can serve as CCN in case they grow to a fixed particle size, which was used in some previous studies, especially for organic-rich environments.

Acknowledgements

The data analysis work done by the first author is supported by National Natural Science Foundation of China (41475127). Data collection was supported by the European Commission projects EUSAAR (European Supersites for Atmospheric Aerosol Research), EUCAARI (European Integrated project on Aerosol Cloud Climate and Air Quality Interactions) FP6-036833-2-EUCAARI, and the German Federal Environment Ministry (BMU) grant F&E 370343200. We acknowledge Friederike Kinder, Andreas Maßling, and Thomas Tuch for their contributions related to H-TDMA and TDMPS data acquisition.

Reference

Altstädter, B., Platis, A., Wehner, B., Scholtz, A., Wildmann, N., Hermann, M., Käthner, R., Baars, H., Bange, J., and Lampert, A.: ALADINA – an unmanned research aircraft for observing vertical and horizontal distributions of ultrafine particles within the atmospheric boundary layer, Atmos. Meas. Tech., 8, 1627-1639, 10.5194/amt-8-1627-2015, 2015.

Asmi, E., Kivekäs, N., Kerminen, V. M., Komppula, M., Hyvärinen, A. P., Hatakka, J., Viisanen, Y., and Lihavainen, H.: Secondary new particle formation in Northern Finland Pallas site between the years 2000 and 2010, Atmos. Chem. Phys., 11, 12959-12972, 10.5194/acp-11-12959-2011, 2011.

Birmili, W., Stratmann, F., and Wiedensohler, A.: Design of a DMA-based size spectrometer for a large particle size range and stable operation, J. Aerosol Sci., 30, 549-553, 1999.

Birmili, W., and Wiedensohler, A.: New particle formation in the continental boundary layer: Meteorological and gas phase parameter influence, Geophysical Research Letters, 27, 3325-3328, 10.1029/1999GL011221, 2000.

Birmili, W., Berresheim, H., Plass-Dülmer, C., Elste, T., Gilge, S., Wiedensohler, A., and Uhrner, U.: The Hohenpeissenberg aerosol formation experiment (HAFEX): a long-term study including size-resolved aerosol, H2SO4, OH, and monoterpenes measurements, Atmos. Chem. Phys., 3, 361-376, 10.5194/acp-3-361-2003, 2003.

Birmili, W., Weinhold, K., Nordmann, S., Wiedensohler, A., Spindler, G., Müller, K., Herrmann, H., Gnauk, T., Pitz, M., Cyrys, J., Flentje, H., Nickel, C., Kuhlbusch, T. A. J., and Löschau, G.: Atmospheric aerosol measurements in the German Ultrafine Aerosol Network (GUAN): Part 1 - soot and particle number size distribution, Gefahrst. Reinh. Luft., 69, 137-145, 2009.

Boy, M., Rannik, Ü., Lehtinen, K. E. J., Tarvainen, V., Hakola, H., and Kulmala, M.: Nucleation events in the continental boundary layer: Long-term statistical analyses of aerosol relevant characteristics, Journal of Geophysical Research: Atmospheres, 108, n/a-n/a, 10.1029/2003JD003838, 2003.

Boy, M., Kulmala, M., Ruuskanen, T. M., Pihlatie, M., Reissell, A., Aalto, P. P., Keronen, P., Dal Maso, M., Hellen, H., Hakola, H., Jansson, R., Hanke, M., and Arnold, F.: Sulphuric acid closure and contribution to nucleation mode particle growth, Atmos. Chem. Phys., 5, 863-878, 10.5194/acp-5-863-2005, 2005.

Boy, M., Hellmuth, O., Korhonen, H., Nilsson, E. D., ReVelle, D., Turnipseed, A., Arnold, F., and Kulmala, M.: MALTE – model to predict new aerosol formation in the lower troposphere, Atmos. Chem. Phys., 6, 4499-4517, 10.5194/acp-6-4499-2006, 2006.

Brus, D., Neitola, K., Hyvärinen, A. P., Petäjä, T., Vanhanen, J., Sipilä, M., Paasonen, P., Kulmala, M., and Lihavainen, H.: Homogenous nucleation of sulfuric acid and water at close to atmospherically relevant conditions, Atmos. Chem. Phys., 11, 5277-5287, 10.5194/acp-11-5277-2011, 2011.

Canagaratna, M. R., Jayne, J. T., Jimenez, J. L., Allan, J. D., Alfarra, M. R., Zhang, Q., Onasch, T. B., Drewnick, F., Coe, H., Middlebrook, A., Delia, A., Williams, L. R., Trimborn, A. M., Northway, M. J., DeCarlo, P. F., Kolb, C. E., Davidovits, P., and Worsnop, D. R.: Chemical and microphysical characterization of ambient aerosols with the aerodyne aerosol mass spectrometer, Mass Spectrometry Reviews, 26, 185-222, 10.1002/mas.20115, 2007.

Cerully, K. M., Raatikainen, T., Lance, S., Tkacik, D., Tiitta, P., Petäjä, T., Ehn, M., Kulmala, M., Worsnop, D. R., Laaksonen, A., Smith, J. N., and Nenes, A.: Aerosol hygroscopicity and CCN activation kinetics in a boreal forest environment during the 2007 EUCAARI campaign, Atmos. Chem. Phys., 11, 12369-12386, 10.5194/acp-11-12369-2011, 2011.

Dal Maso, M., Kulmala, M., Riipinen, I., Wagner, R., Hussein, T., Aalto, P. P., and Lehtinen, K. E.: Formation and growth of fresh atmospheric aerosols: eight years of aerosol size distribution data from SMEAR II, Hyytiala, Finland, Boreal Environment Research, 10, 323, 2005.

DeCarlo, P. F., Kimmel, J. R., Trimborn, A., Northway, M. J., Jayne, J. T., Aiken, A. C., Gonin, M., Fuhrer, K., Horvath, T., Docherty, K. S., Worsnop, D. R., and Jimenez, J. L.: Field-Deployable, High-Resolution, Time-of-Flight Aerosol Mass Spectrometer, Analytical Chemistry, 78, 8281-8289, 10.1021/ac061249n, 2006.

Dusek, U., Frank, G. P., Hildebrandt, L., Curtius, J., Schneider, J., Walter, S., Chand, D., Drewnick, F., Hings, S., Jung, D., Borrmann, S., and Andreae, M. O.: Size Matters More Than Chemistry for Cloud-Nucleating Ability of Aerosol Particles, Science, 312, 1375-1378, 10.1126/science.1125261, 2006.

Dusek, U., Frank, G. P., Curtius, J., Drewnick, F., Schneider, J., Kürten, A., Rose, D., Andreae, M. O., Borrmann, S., and Pöschl, U.: Enhanced organic mass fraction and decreased hygroscopicity of cloud condensation nuclei (CCN) during new particle formation events, Geophysical Research Letters, 37, n/a-n/a, 10.1029/2009GL040930, 2010.

Ehn, M., Petäjä, T., Aufmhoff, H., Aalto, P., Hämeri, K., Arnold, F., Laaksonen, A., and Kulmala, M.: Hygroscopic properties of ultrafine aerosol particles in the boreal forest: diurnal variation, solubility and the influence of sulfuric acid, Atmos. Chem. Phys., 7, 211-222, 10.5194/acp-7-211-2007, 2007.

Good, N., Topping, D. O., Allan, J. D., Flynn, M., Fuentes, E., Irwin, M., Williams, P. I., Coe, H., and McFiggans, G.: Consistency between parameterisations of aerosol hygroscopicity and CCN activity during the RHaMBLe discovery cruise, Atmos. Chem. Phys., 10, 3189-3203, 10.5194/acp-10-3189-2010, 2010.

Größ, J., Birmili, W., Hamed, A., Sonntag, A., Wiedensohler, A., Spindler, G., Maninnen, H. E., Nieminen, T., Kulmala, M., Hõrrak, U., and Plass-Dülmer, C.: Evolution of gaseous precursors and meteorological parameters during new particle formation events in the Central European boundary layer, Atmos. Chem. Phys. Discuss., 15, 2305-2353, 10.5194/acpd-15-2305-2015, 2015.

Gysel, M., Crosier, J., Topping, D. O., Whitehead, J. D., Bower, K. N., Cubison, M. J., Williams, P. I., Flynn, M. J., McFiggans, G. B., and Coe, H.: Closure study between chemical composition and hygroscopic growth of aerosol particles during TORCH2, Atmos. Chem. Phys., 7, 6131-6144, 10.5194/acp-7-6131-2007, 2007.

Gysel, M., McFiggans, G. B., and Coe, H.: Inversion of tandem differential mobility analyser (TDMA) measurements, Journal of Aerosol Science, 40, 134-151, 10.1016/j.jaerosci.2008.07.013, 2009.

Hämeri, K., Väkevä, M., Aalto, P. P., Kulmala, M., Swietlicki, E., Zhou, J., Seidl, W., Becker, E., and O'Dowd, C. D.: Hygroscopic and CCN properties of aerosol particles in boreal forests, Tellus B, 53, 359-379, 10.1034/j.1600-0889.2001.530404.x, 2001.

Hamed, A., Birmili, W., Joutsensaari, J., Mikkonen, S., Asmi, A., Wehner, B., Spindler, G., Jaatinen, A., Wiedensohler, A., Korhonen, H., Lehtinen, K. E. J., and Laaksonen, A.: Changes in the production rate of secondary aerosol particles in Central Europe in view of decreasing SO2 emissions between 1996 and 2006, Atmos. Chem. Phys., 10, 1071-1091, 10.5194/acp-10-1071-2010, 2010.

Heintzenberg, J.: Properties of the Log-Normal Particle Size Distribution, Aerosol Science and Technology, 21, 46-48, 10.1080/02786829408959695, 1994.

Hussein, T., Aalto, P. P., and Lehtinen, K. E. J.: Formation and growth of fresh atmospheric aerosols: eight years of aerosol size distribution data from SMEAR II, Hyytiälä, Finland, 2000.

Irwin, M., Good, N., Crosier, J., Choularton, T. W., and McFiggans, G.: Reconciliation of measurements of hygroscopic growth and critical supersaturation of aerosol particles in central Germany, Atmos. Chem. Phys., 10, 11737-11752, 10.5194/acp-10-11737-2010, 2010.

Janhäll, S., M. Jonsson, Å., Molnár, P., A. Svensson, E., and Hallquist, M.: Size resolved traffic emission factors of submicrometer particles, Atmospheric Environment, 38, 4331-4340, http://dx.doi.org/10.1016/j.atmosenv.2004.04.018, 2004.

Kazil, J., Stier, P., Zhang, K., Quaas, J., Kinne, S., O'Donnell, D., Rast, S., Esch, M., Ferrachat, S., Lohmann, U., and Feichter, J.: Aerosol nucleation and its role for clouds and Earth's radiative forcing in the aerosol-climate model ECHAM5-HAM, Atmos. Chem. Phys., 10, 10733-10752, 10.5194/acp-10-10733-2010, 2010.

Kerminen, V.-M., Lehtinen, K. E. J., Anttila, T., and Kulmala, M.: Dynamics of atmospheric nucleation mode particles: a timescale analysis, Tellus B, 56, 135–146, 10.3402/tellusb.v56i2.16411, 2004.

Kerminen, V. M., Paramonov, M., Anttila, T., Riipinen, I., Fountoukis, C., Korhonen, H., Asmi, E., Laakso, L., Lihavainen, H., Swietlicki, E., Svenningsson, B., Asmi, A., Pandis, S. N., Kulmala, M., and Petäjä, T.: Cloud condensation nuclei production associated with atmospheric nucleation: a synthesis based on existing literature and new results, Atmos. Chem. Phys., 12, 12037-12059, 10.5194/acp-12-12037-2012, 2012.

Kiendler-Scharr, A., Wildt, J., Maso, M. D., Hohaus, T., Kleist, E., Mentel, T. F., Tillmann, R., Uerlings, R., Schurr, U., and Wahner, A.: New particle formation in forests inhibited by isoprene emissions, Nature, 461, 381-384, http://www.nature.com/nature/journal/v461/n7262/suppinfo/nature08292_S1.html, 2009.

Kuang, C., McMurry, P. H., and McCormick, A. V.: Determination of cloud condensation nuclei production from measured new particle formation events, Geophysical Research Letters, 36, L09822, 10.1029/2009GL037584, 2009.

Kulmala, M., Laakso, L., Lehtinen, K. E. J., Riipinen, I., Dal Maso, M., Anttila, T., Kerminen, V. M., Hõrrak, U., Vana, M., and Tammet, H.: Initial steps of aerosol growth, Atmos. Chem. Phys., 4, 2553-2560, 10.5194/acp-4-2553-2004, 2004.

Kulmala, M., Lehtinen, K. E. J., and Laaksonen, A.: Cluster activation theory as an explanation of the linear dependence between formation rate of 3nm particles and sulphuric acid concentration, Atmos. Chem. Phys., 6, 787-793, 10.5194/acp-6-787-2006, 2006.

Kulmala, M., Asmi, A., Lappalainen, H. K., Carslaw, K. S., Pöschl, U., Baltensperger, U., Hov, Ø., Brenquier, J. L., Pandis, S. N., Facchini, M. C., Hansson, H. C., Wiedensohler, A., and O'Dowd, C. D.: Introduction: European Integrated Project on Aerosol Cloud Climate and Air Quality interactions (EUCAARI) – integrating aerosol research from nano to global scales, Atmos. Chem. Phys., 9, 2825-2841, 10.5194/acp-9-2825-2009, 2009.

Kulmala, M., Petäjä, T., Nieminen, T., Sipilä, M., Manninen, H. E., Lehtipalo, K., Dal Maso, M., Aalto, P. P., Junninen, H., Paasonen, P., Riipinen, I., Lehtinen, K. E. J., Laaksonen, A., and Kerminen, V.-M.: Measurement of the nucleation of atmospheric aerosol particles, Nat. Protocols, 7, 1651-1667, http://www.nature.com/nprot/journal/v7/n9/abs/nprot.2012.091.html#supplementary-information, 2012.

Kurtén, T., Torpo, L., Ding, C.-G., Vehkamäki, H., Sundberg, M. R., Laasonen, K., and Kulmala, M.: A density functional study on water-sulfuric acid-ammonia clusters and implications for atmospheric cluster formation, Journal of Geophysical Research: Atmospheres, 112, n/a-n/a, 10.1029/2006jd007391, 2007.

Laakso, L., Petäjä, T., Lehtinen, K. E. J., Kulmala, M., Paatero, J., Hõrrak, U., Tammet, H., and Joutsensaari, J.: Ion production rate in a boreal forest based on ion, particle and radiation measurements, Atmos. Chem. Phys., 4, 1933-1943, 10.5194/acp-4-1933-2004, 2004.

Laakso, L., Merikanto, J., Vakkari, V., Laakso, H., Kulmala, M., Molefe, M., Kgabi, N., Mabaso, D., Carslaw, K. S., Spracklen, D. V., Lee, L. A., Reddington, C. L., and Kerminen, V. M.: Boundary layer nucleation as a source of new CCN in savannah environment, Atmos. Chem. Phys., 13, 1957-1972, 10.5194/acp-13-1957-2013, 2013.

Laaksonen, A., Hamed, A., Joutsensaari, J., Hiltunen, L., Cavalli, F., Junkermann, W., Asmi, A., Fuzzi, S., and Facchini, M. C.: Cloud condensation nucleus production from nucleation events at a highly polluted region, Geophys. Res. Lett., 32, L06812, 10.1029/2004gl022092, 2005.

Malm, W. C., and Kreidenweis, S. M.: The effects of models of aerosol hygroscopicity on the apportionment of extinction, Atmospheric Environment, 31, 1965-1976, 10.1016/s1352-2310(96)00355-x, 1997.

Massling, A., Wiedensohler, A., Busch, B., Neusüß, C., Quinn, P., Bates, T., and Covert, D.: Hygroscopic properties of different aerosol types over the Atlantic and Indian Oceans, Atmos. Chem. Phys., 3, 1377-1397, 10.5194/acp-3-1377-2003, 2003.

Massling, A., Niedermeier, N., Hennig, T., Fors, E. O., Swietlicki, E., Ehn, M., Hämeri, K., Villani, P., Laj, P., Good, N., McFiggans, G., and Wiedensohler, A.: Results and recommendations from an intercomparison of six Hygroscopicity-TDMA systems, Atmos. Meas. Tech., 4, 485-497, 10.5194/amt-4-485-2011, 2011.

Merikanto, J., Spracklen, D. V., Mann, G. W., Pickering, S. J., and Carslaw, K. S.: Impact of nucleation on global CCN, Atmos. Chem. Phys., 9, 8601-8616, 10.5194/acp-9-8601-2009, 2009.

Mutzel, A., Poulain, L., Berndt, T., Iinuma, Y., Rodigast, M., Böge, O., Richters, S., Spindler, G., Sipilä, M., Jokinen, T., Kulmala, M., and Herrmann, H.: Highly Oxidized Multifunctional Organic Compounds Observed in Tropospheric Particles: A Field and Laboratory Study, Environmental Science & Technology, 49, 7754-7761, 10.1021/acs.est.5b00885, 2015.

Nieminen, T., Lehtinen, K. E. J., and Kulmala, M.: Sub-10 nm particle growth by vapor condensation – effects of vapor molecule size and particle thermal speed, Atmos. Chem. Phys., 10, 9773-9779, 10.5194/acp-10-9773-2010, 2010.

Paasonen, P., Nieminen, T., Asmi, E., Manninen, H. E., Petäjä, T., Plass-Dülmer, C., Flentje, H., Birmili, W., Wiedensohler, A., Hõrrak, U., Metzger, A., Hamed, A., Laaksonen, A., Facchini, M. C., Kerminen, V. M., and Kulmala, M.: On the roles of sulphuric acid and low-volatility organic vapours in the initial steps of atmospheric new particle formation, Atmos. Chem. Phys., 10, 11223-11242, 10.5194/acp-10-11223-2010, 2010.

Paasonen, P., Asmi, A., Petaja, T., Kajos, M. K., Aijala, M., Junninen, H., Holst, T., Abbatt, J. P. D., Arneth, A., Birmili, W., van der Gon, H. D., Hamed, A., Hoffer, A., Laakso, L., Laaksonen, A., Richard Leaitch, W., Plass-Dulmer, C., Pryor, S. C., Raisanen, P., Swietlicki, E., Wiedensohler, A., Worsnop, D. R., Kerminen, V.-M., and Kulmala, M.: Warming-induced increase in aerosol number concentration likely to moderate climate change, Nature Geosci, 6, 438-442, 10.1038/ngeo1800

http://www.nature.com/ngeo/journal/v6/n6/abs/ngeo1800.html#supplementary-information, 2013.

Petters, M. D., and Kreidenweis, S. M.: A single parameter representation of hygroscopic growth and cloud condensation nucleus activity, Atmos. Chem. Phys., 7, 1961-1971, 10.5194/acp-7-1961-2007, 2007.

Petters, M. D., Wex, H., Carrico, C. M., Hallbauer, E., Massling, A., McMeeking, G. R., Poulain, L., Wu, Z., Kreidenweis, S. M., and Stratmann, F.: Towards closing the gap between hygroscopic growth and activation for secondary organic aerosol – Part 2: Theoretical approaches, Atmos. Chem. Phys., 9, 3999-4009, 10.5194/acp-9-3999-2009, 2009.

Pierce, J. R., Riipinen, I., Kulmala, M., Ehn, M., Petäjä, T., Junninen, H., Worsnop, D. R., and Donahue, N. M.: Quantification of the volatility of secondary organic compounds in ultrafine particles during nucleation events, Atmos. Chem. Phys., 11, 9019-9036, 10.5194/acp-11-9019-2011, 2011.

Pirjola, L., Kulmala, M., Wilck, M., Bischoff, A., Stratmann, F., and Otto, E.: FORMATION OF SULPHURIC ACID AEROSOLS AND CLOUD CONDENSATION NUCLEI: AN EXPRESSION FOR SIGNIFICANT NUCLEATION AND MODEL COMPRARISON, Journal of Aerosol Science, 30, 1079-1094, http://dx.doi.org/10.1016/S0021-8502(98)00776-9, 1999.

Potukuchi, S., and Wexler, A. S.: Identifying solid-aqueous phase transitions in atmospheric aerosols—I. Neutral-acidity solutions, Atmospheric Environment, 29, 1663-1676, http://dx.doi.org/10.1016/1352-2310(95)00074-9, 1995.

Poulain, L., Birmili, W., Canonaco, F., Crippa, M., Wu, Z. J., Nordmann, S., Spindler, G., Prévôt, A. S. H., Wiedensohler, A., and Herrmann, H.: Chemical mass balance of 300 °C non-volatile particles at the tropospheric research site Melpitz, Germany, Atmos. Chem. Phys., 14, 10145-10162, 10.5194/acp-14-10145-2014, 2014.

Ristovski, Z. D., Suni, T., Kulmala, M., Boy, M., Meyer, N. K., Duplissy, J., Turnipseed, A., Morawska, L., and Baltensperger, U.: The role of sulphates and organic vapours in growth of newly formed particles in a eucalypt forest, Atmos. Chem. Phys., 10, 2919-2926, 10.5194/acp-10-2919-2010, 2010.

Sihto, S. L., Mikkilä, J., Vanhanen, J., Ehn, M., Liao, L., Lehtipalo, K., Aalto, P. P., Duplissy, J., Petäjä, T., Kerminen, V. M., Boy, M., and Kulmala, M.: Seasonal variation of CCN concentrations and aerosol activation properties in boreal forest, Atmos. Chem. Phys., 11, 13269-13285, 10.5194/acp-11-13269-2011, 2011.

Sipilä, M., Berndt, T., Petäjä, T., Brus, D., Vanhanen, J., Stratmann, F., Patokoski, J., Mauldin, R. L., Hyvärinen, A.-P., Lihavainen, H., and Kulmala, M.: The Role of Sulfuric Acid in Atmospheric Nucleation, Science, 327, 1243-1246, 2010.

Smith, J. N., Moore, K. F., McMurry, P. H., and Eisele, F. L.: Atmospheric Measurements of Sub-20 nm Diameter Particle Chemical Composition by Thermal Desorption Chemical Ionization Mass Spectrometry, Aerosol Science and Technology, 38, 100-110, 10.1080/02786820490249036, 2004.

Sotiropoulou, R. E. P., Tagaris, E., Pilinis, C., Anttila, T., and Kulmala, M.: Modeling New Particle Formation During Air Pollution Episodes: Impacts on Aerosol and Cloud Condensation Nuclei, Aerosol Science and Technology, 40, 557-572, 10.1080/02786820600714346, 2006.

Spracklen, D. V., Carslaw, K. S., Kulmala, M., Kerminen, V.-M., Sihto, S.-L., Riipinen, I., Merikanto, J., Mann, G. W., Chipperfield, M. P., Wiedensohler, A., Birmili, W., and Lihavainen, H.: Contribution of particle formation to global cloud condensation nuclei concentrations, Geophys. Res. Lett., 35, L06808, 10.1029/2007gl033038, 2008.

Stokes, R. H., and Robinson, R. A.: Interactions in Aqueous Nonelectrolyte Solutions. I. Solute-Solvent Equilibria, Journal of Physical Chemistry, 70, 2126-2130, 1966.

Stolzenburg, M. R., McMurry, P. H., Sakurai, H., Smith, J. N., Mauldin, R. L., Eisele, F. L., and Clement, C. F.: Growth rates of freshly nucleated atmospheric particles in Atlanta, Journal of Geophysical Research: Atmospheres, 110, D22S05, 10.1029/2005JD005935, 2005.

Swietlicki, E., Zhou, J., Berg, O. H., Martinsson, B. G., Frank, G., Cederfelt, S.-I., Dusek, U., Berner, A., Birmili, W., Wiedensohler, A., Yuskiewicz, B., and Bower, K. N.: A closure study of sub-micrometer aerosol particle hygroscopic behaviour, Atmospheric Research, 50, 205-240, 10.1016/s0169-8095(98)00105-7, 1999.

Tang, I. N., and Munkelwitz, H. R.: Water activities, densities, and refractive indices of aqueous sulfates and sodium nitrate droplets of atmospheric importance, J. Geophys. Res., 99, 18801-18808, 10.1029/94jd01345, 1994.

Tuch, T. M., Haudek, A., Müller, T., Nowak, A., Wex, H., and Wiedensohler, A.: Design and performance of an automatic regenerating adsorption aerosol dryer for continuous operation at monitoring sites, Atmos. Meas. Tech., 2, 417-422, 2009.

Varutbangkul, V., Brechtel, F. J., Bahreini, R., Ng, N. L., Keywood, M. D., Kroll, J. H., Flagan, R. C., Seinfeld, J. H., Lee, A., and Goldstein, A. H.: Hygroscopicity of secondary organic aerosols formed by oxidation of cycloalkenes, monoterpenes, sesquiterpenes, and related compounds, Atmos. Chem. Phys., 6, 2367-2388, 10.5194/acp-6-2367-2006, 2006.

Virkkula, A., Van Dingenen, R., Raes, F., and Hjorth, J.: Hygroscopic properties of aerosol formed by oxidation of limonene, α-pinene, and β-pinene, J. Geophys. Res., 104, 3569-3579, 10.1029/1998jd100017, 1999.

Wang, L., Khalizov, A. F., Zheng, J., Xu, W., Ma, Y., Lal, V., and Zhang, R.: Atmospheric nanoparticles formed from heterogeneous reactions of organics, Nature Geosci, 3, 238-242, http://www.nature.com/ngeo/journal/v3/n4/suppinfo/ngeo778_S1.html, 2010.

Wang, M., and Penner, J. E.: Aerosol indirect forcing in a global model with particle nucleation, Atmos. Chem. Phys., 9, 239-260, 10.5194/acp-9-239-2009, 2009.

Weber, R. J., Marti, J. J., McMurry, P. H., Eisele, F. L., Tanner, D. J., and Jefferson, A.: Measurements of new particle formation and ultrafine particle growth rates at a clean continental site, Journal of Geophysical Research: Atmospheres, 102, 4375-4385, 10.1029/96JD03656, 1997.

Westervelt, D. M., Pierce, J. R., and Adams, P. J.: Analysis of feedbacks between nucleation rate, survival probability and cloud condensation nuclei formation, Atmos. Chem. Phys., 14, 5577-5597, 10.5194/acp-14-5577-2014, 2014.

Wex, H., Petters, M. D., Carrico, C. M., Hallbauer, E., Massling, A., McMeeking, G. R., Poulain, L., Wu, Z., Kreidenweis, S. M., and Stratmann, F.: Towards closing the gap between hygroscopic growth and activation for secondary organic aerosol: Part 1 – Evidence from measurements, Atmos. Chem. Phys., 9, 3987-3997, 10.5194/acp-9-3987-2009, 2009.

Wiedensohler, A., Cheng, Y. F., Nowak, A., Wehner, B., Achtert, P., Berghof, M., Birmili, W., Wu, Z. J., Hu, M., Zhu, T., Takegawa, N., Kita, K., Kondo, Y., Lou, S. R., Hofzumahaus, A., Holland, F., Wahner, A., Gunthe, S. S., Rose, D., Su, H., and Pöschl, U.: Rapid aerosol particle growth and increase of cloud condensation nucleus activity by secondary aerosol formation and condensation: A case study for regional air pollution in northeastern China, J. Geophys. Res., 114, D00G08, 10.1029/2008jd010884, 2009.

Wiedensohler, A., Birmili, W., Nowak, A., Sonntag, A., Weinhold, K., Merkel, M., Wehner, B., Tuch, T., Pfeifer, S., Fiebig, M., Fjaraa, A. M., Asmi, E., Sellegri, K., Depuy, R., Venzac, H., Villani, P., Laj, P., Aalto, P., Ogren, J. A., Swietlicki, E., Williams, P., Roldin, P., Quincey, P., Huglin, C., Fierz-Schmidhauser, R., Gysel, M., Weingartner, E., Riccobono, F., Santos, S., Gruning, C., Faloon, K., Beddows, D., Harrison, R. M., Monahan, C., Jennings, S. G., O'Dowd, C. D., Marinoni, A., Horn, H. G., Keck, L., Jiang, J., Scheckman, J., McMurry, P. H., Deng, Z., Zhao, C. S., Moerman, M., Henzing, B., de Leeuw, G., Loschau, G., and Bastian, S.: Mobility particle size spectrometers: harmonization of technical standards and data structure to facilitate high quality long-term observations of atmospheric particle number size distributions, Atmos. Meas. Tech., 5, 657-685, DOI 10.5194/amt-5-657-2012, 2012.

Wu, Z. J., Nowak, A., Poulain, L., Herrmann, H., and Wiedensohler, A.: Hygroscopic behavior of atmospherically relevant water-soluble carboxylic salts and their influence on the water uptake of ammonium sulfate, Atmos. Chem. Phys., 11, 12617-12626, 10.5194/acp-11-12617-2011, 2011.

Wu, Z. J., Poulain, L., Henning, S., Dieckmann, K., Birmili, W., Merkel, M., van Pinxteren, D., Spindler, G., Mueller, K., Stratmann, F., Herrmann, H., and Wiedensohler, A.: Relating particle hygroscopicity and CCN activity to chemical composition during the HCCT-2010 field campaign, Atmospheric Chemistry and Physics, 13, 7983-7996, 10.5194/acp-13-7983-2013, 2013.

Yue, D. L., Hu, M., Zhang, R. Y., Wang, Z. B., Zheng, J., Wu, Z. J., Wiedensohler, A., He, L. Y., Huang, X. F., and Zhu, T.: The roles of sulfuric acid in new particle formation and growth in the mega-city of Beijing, Atmos. Chem. Phys., 10, 4953-4960, DOI 10.5194/acp-10-4953-2010, 2010.

Yue, D. L., Hu, M., Zhang, R. Y., Wu, Z. J., Su, H., Wang, Z. B., Peng, J. F., He, L. Y., Huang, X. F., Gong, Y. G., and Wiedensohler, A.: Potential contribution of new particle formation to cloud condensation nuclei in Beijing, Atmospheric Environment, 45, 6070-6077, http://dx.doi.org/10.1016/j.atmosenv.2011.07.037, 2011.

Zdanovskii, B.: Novyi Metod Rascheta Rastvorimostei Elektrolitov v Mnogokomponentnykh Sistema, , Zh. Fiz. Khim+, 22, 1478-1485, 1486-1495, 1948.

Zhang, Q., Stanier, C. O., Canagaratna, M. R., Jayne, J. T., Worsnop, D. R., Pandis, S. N., and Jimenez, J. L.: Insights into the Chemistry of New Particle Formation and Growth Events in Pittsburgh Based on Aerosol Mass Spectrometry, Environmental Science & Technology, 38, 4797-4809, 10.1021/es035417u, 2004a.

Zhang, R., Suh, I., Zhao, J., Zhang, D., Fortner, E. C., Tie, X., Molina, L. T., and Molina, M. J.: Atmospheric New Particle Formation Enhanced by Organic Acids, Science, 304, 1487-1490, 10.1126/science.1095139, 2004b.

Zhu, Y., Hinds, W. C., Kim, S., and Sioutas, C.: Concentration and Size Distribution of Ultrafine Particles Near a Major Highway, Journal of the Air & Waste Management Association, 52, 1032-1042, 10.1080/10473289.2002.10470842, 2002.

Tables and figures

Table 1: The summary of instruments and parameters used in this study.

Instrument	Parameter
SMPS	Particle number size distribution
H-TDMA	Particle hygroscopicity
HR-ToF-AMS	Size-resolved chemical composition
Monitor – APSA 360 Horiba Europe	SO_2 concentration
Kipp & Zonen CM6 Pyranometer	Global solar irradiance

Table 2: Gravimetric densities ρ and hygroscopicity parameters κ.

Species	NH_4NO_3	H_2SO_4	NH_4HSO_4	$(NH_4)_2SO_4$	Organic matter
ρ [kg/m^3]	1720	1830	1780	1769	1400
κ	0.67	0.92	0.61	0.61	0.1

Table 3: The water soluble fraction of newly formed particles and the ratios of H_2SO_4 condensational growth to the observed particle growth

Dp	35 nm		50 nm		75 nm	
Date	ε	$F_{GR_{H_2SO_4}}$ *	ε	$F_{GR_{H_2SO_4}}$	ε	$F_{GR_{H_2SO_4}}$
05-06-2008	--		24%	23%	20%	15%
06-06-2008	25%	23%	14%	17%	10%	11%
07-06-2008	34%	30%	23%	20%	17%	13%

* $F_{GR_{H_2SO_4}}=GR_{H_2SO_4}/GR_{obs}$: The ratio of H_2SO_4 condensational growth to the observed particle growth. Here, GR_{obs}s for 35, 50, and 75 nm were calculated over the time period during which mean geometric diameter of log-normal ultrafine particle mode grew to 35, 50, and 75 nm, respectively, as indicated by the white circles in the Fig.1 (a).

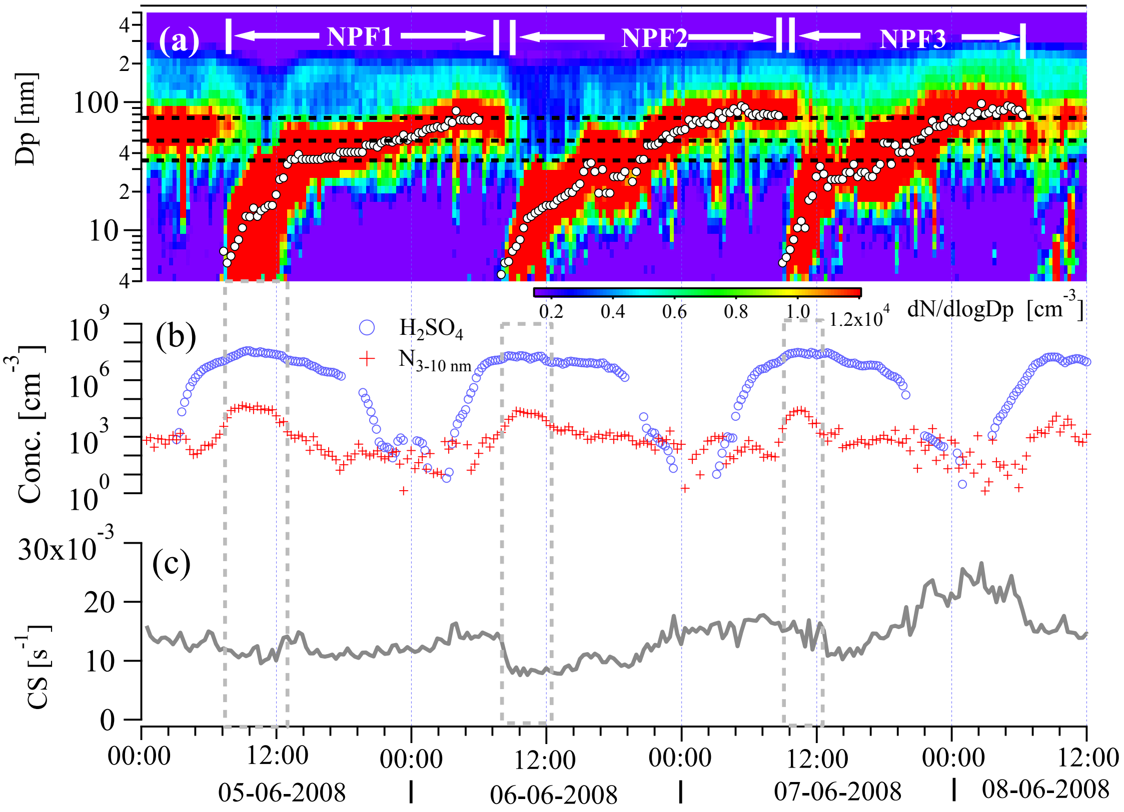

Fig. 1: Particle number size distribution (a), 3-10 nm particle number concentration and H_2SO_4 concentration (b), condensation sink (CS) (c) during the NPF events. The starting and ending time of the events were marked in the upper place of panel (a) by NPF1, NPF2, and NPF3. The while circles in the panel (a) are the D_m of new particles modes. The grey dashed lines indicated the time period of particle formation.

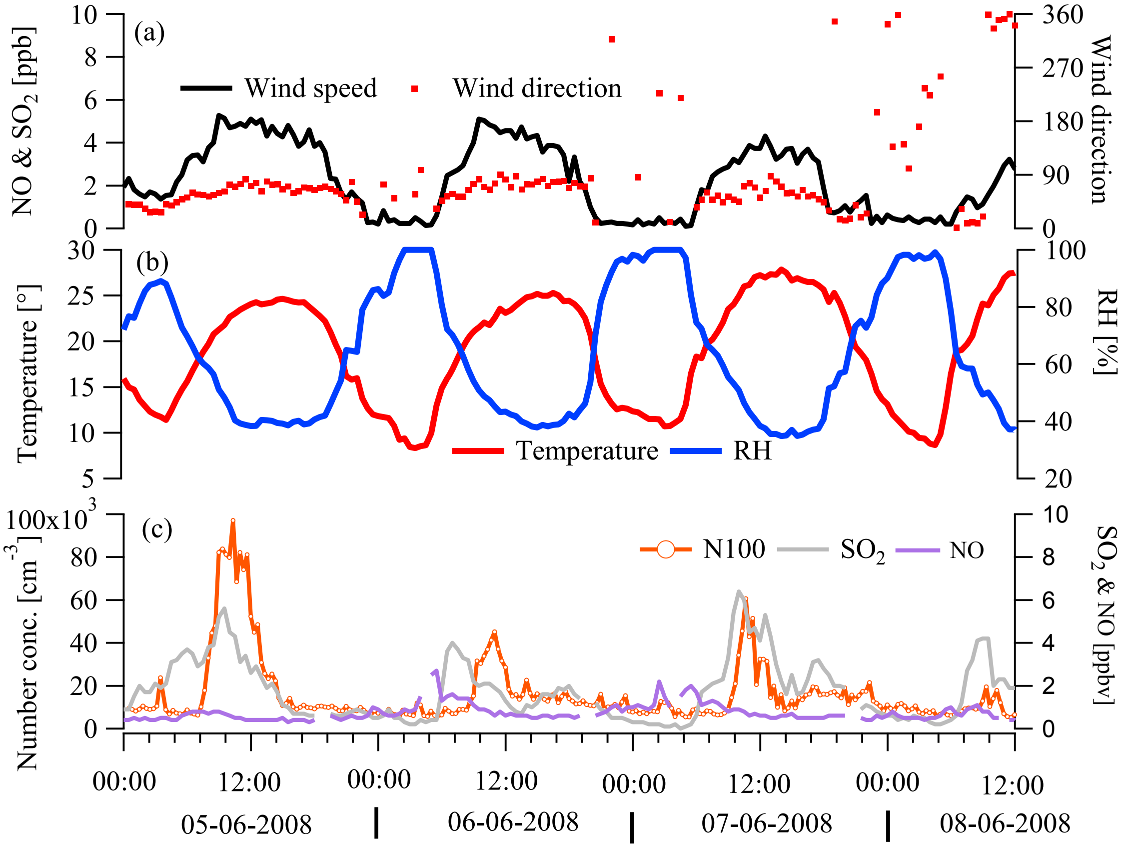

Fig. 2: The time series of wind speed and wind direction (a), ambient temperature and RH (b), and SO_2 & NO concentrations and number concentrations of particles in diameters of 3-100 nm (b).

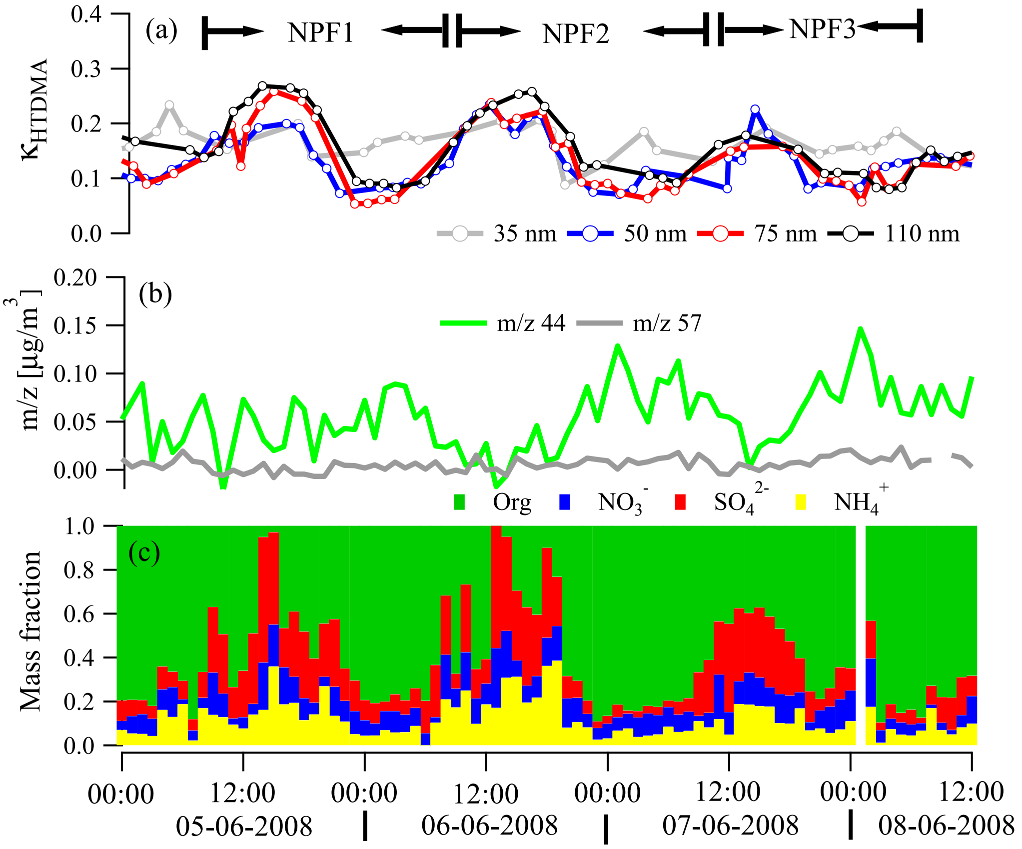

Fig.3: Size-resolved particle hygroscopicity (a), m/z 44 and 57 mass concentrations in 30-100 nm particles (b), and mass fraction of organic, sulfate, nitrate, and ammonium in 30-100 nm particles (c).

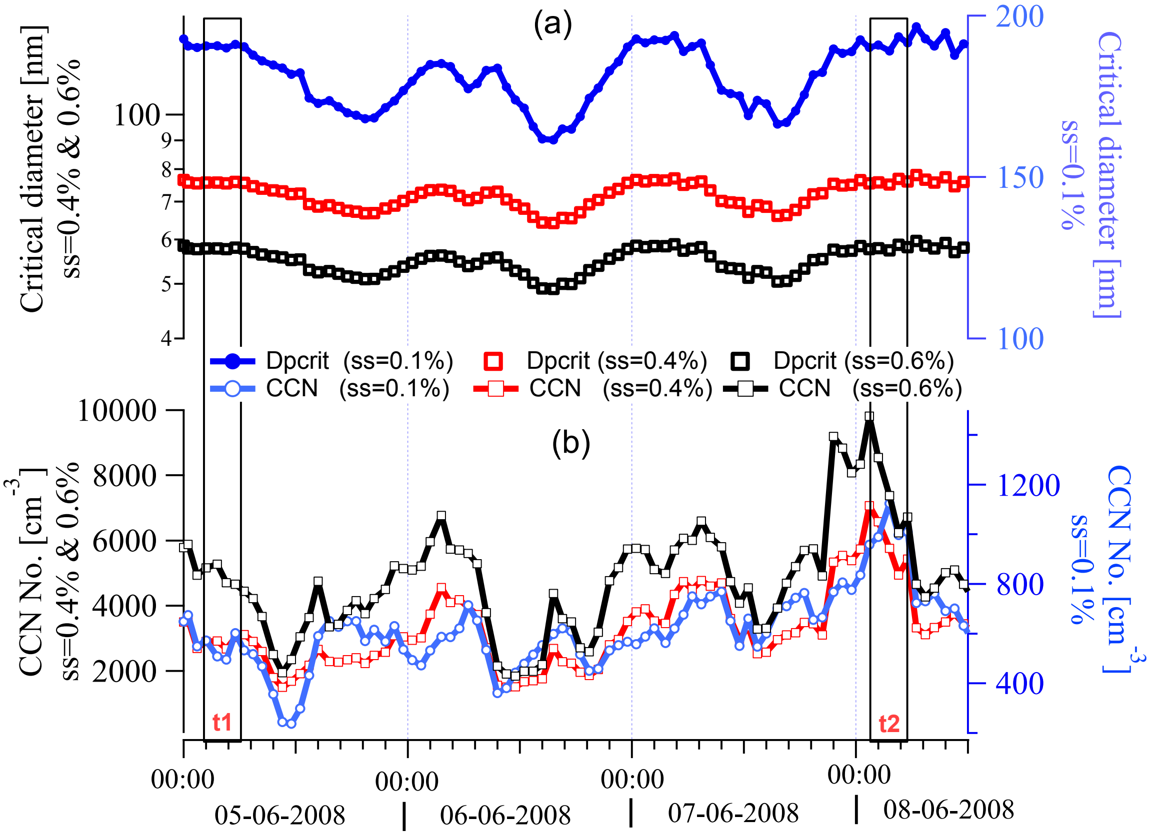

Fig. 4: Critical diameter (Dpcrit) and CCN number concentration during NPF events.